

The Science and Technology of Rubber

Fourth Edition

Edited by

Burak Erman

Department of Chemical and Biological Engineering
Koc University
Rumeli Feneri Yolu 34450 Istanbul, Turkey

James E. Mark

Department of Chemistry
University of Cincinnati
Cincinnati, OH 45221-0172, USA

C. Michael Roland

Naval Research Laboratory
Chemistry Division, Code 6120
Washington, DC, USA



ELSEVIER

AMSTERDAM • BOSTON • HEIDELBERG • LONDON
NEW YORK • OXFORD • PARIS • SAN DIEGO
SAN FRANCISCO • SINGAPORE • SYDNEY • TOKYO

Academic Press is an Imprint of Elsevier



Academic Press is an imprint of Elsevier
225 Wyman Street, Waltham, MA 02451, USA
The Boulevard, Langford Lane, Kidlington, Oxford, OX5 1GB, UK

© 2013 Elsevier Inc. All rights reserved.

No part of this publication may be reproduced or transmitted in any form or by any means, electronic or mechanical, including photocopying, recording, or any information storage and retrieval system, without permission in writing from the publisher. Details on how to seek permission, further information about the Publisher's permissions policies and our arrangements with organizations such as the Copyright Clearance Center and the Copyright Licensing Agency, can be found at our website: www.elsevier.com/permissions.

This book and the individual contributions contained in it are protected under copyright by the Publisher (other than as may be noted herein).

Notices

Knowledge and best practice in this field are constantly changing. As new research and experience broaden our understanding, changes in research methods, professional practices, or medical treatment may become necessary.

Practitioners and researchers must always rely on their own experience and knowledge in evaluating and using any information, methods, compounds, or experiments described herein. In using such information or methods they should be mindful of their own safety and the safety of others, including parties for whom they have a professional responsibility.

To the fullest extent of the law, neither the Publisher nor the authors, contributors, or editors, assume any liability for any injury and/or damage to persons or property as a matter of products liability, negligence or otherwise, or from any use or operation of any methods, products, instructions, or ideas contained in the material herein.

Library of Congress Cataloging-in-Publication Data

A catalog record for this book is available from the Library of Congress

British Library Cataloguing-in-Publication Data

A catalogue record for this book is available from the British Library.

ISBN: 978-0-12-394584-6

For information on all Academic Press publications
visit our website at <http://store.elsevier.com>

Printed in the United States of America

13 14 15 9 8 7 6 5 4 3 2 1



Rheological Behavior and Processing of Unvulcanized Rubber

C.M Roland

Chemistry Division, Naval Research Laboratory, Washington, DC, USA

6.1 RHEOLOGY

6.1.1 Introduction

The mixing and processing of rubber is centrally important to achieving useful products at acceptable cost. Various texts review the general topic of polymer processing (Osswald and Gries, 2006; Baird and Collias, 1998; Morton-Jones, 1989; Tadmor and Gogos, 2006) and the rheology and viscoelasticity of rubbery polymers (Roland, 2011; Macosko, 1994; Ferry, 1980; Watanabe, 1999; Berry, 2003; Graessley, 2008), including some specific to rubber processing (White, 1995; Johnson, 2001). This chapter provides a basic overview of the rheology (from the Greek *rheos*, meaning stream or flow, rheology is the study of the deformation and flow of matter) and processing of uncured rubber, including recent developments concerning the material behavior.

The study of the rheology and processing of rubber had its beginnings with the development of the industry in the early 19th century (Hancock, 1920). A major advance was the Boltzmann superposition principle (Boltzmann, 1874) (Section 6.2.2), enabling prediction of stresses in a material subjected to arbitrary strain histories. Early elastic recoil data of Mooney on natural rubber (Mooney, 1936) are displayed in Figure 6.1, illustrating the Boltzmann superpositioning: A short time delay in the onset of recovery only affects the recovery at short times; the behavior over longer times is essentially the same. The first experimental measurements of viscoelastic behavior were on silk thread, carried out in the mid-19th century (Weber, 1835), although there is an oblique reference to the concept in the biblical book of Judges 5:5,

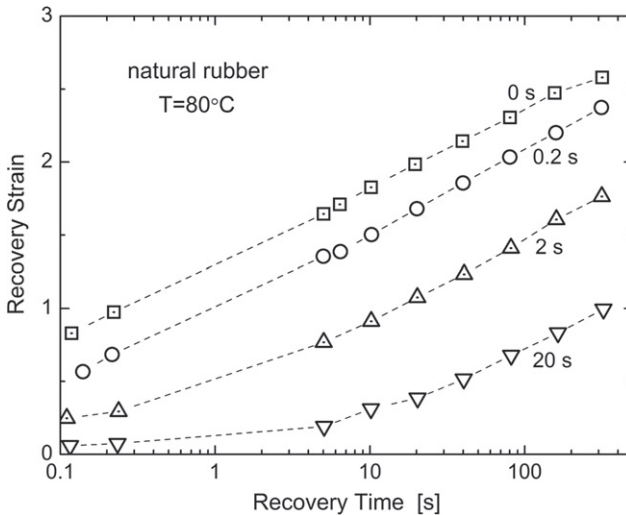


FIGURE 6.1 Elastic recovery of natural rubber following imposition of a strain for the indicated time period. The initial recovery is reduced by maintaining the material in the stretched condition, but the recovery at longer times is unaffected (Mooney, 1936).

“*The mountains flow before the Lord,*” expressing the idea that even solids exhibit viscous behavior over a sufficiently long time frame.

The first recorded processing of rubber is attributed to the Olmec, the earliest major civilization in Mexico. Analysis of excavated rubber balls dating to 1600 BC indicates that the Olmec heated a mixture of rubber latex with liquid extracted from *Ipomoea Alba*, a species of morning glory vine (Hosler et al., 1999). The process removes nonpolymeric contaminants from the 1,4-polyisoprene and probably introduces low levels of crosslinking. Evidently the resulting rubber balls had sufficient shape retention and elasticity to be used for games. This material was possibly used also for waterproofing (Wendt and Cyphers, 2008). About 3400 years later, Macintosh Hancock (1920) coated woven fabrics with solutions of rubber for the same purpose, leading to early manufacture of raincoats bearing the inventor’s name. About 20 years later Goodyear invented the process of sulfur vulcanization of rubber, which became universally adopted and enabled most modern applications (Reader’s Digest, 1958).

6.1.2 Basic Concepts

The mechanical response of a material is described by constitutive equations, which are geometry-independent, but usually limited to specific conditions of temperature, pressure, and even type of deformation. Hooke’s law describes the response to a tensile strain ε :

$$\sigma = E\varepsilon \quad (6.1)$$

in which σ is the stress and E is a material constant known as Young's modulus. For a strictly elastic material, the behavior is reversible. The behavior of sheared fluids can be described by an equation due to Newton:

$$\sigma = \eta \dot{\epsilon} \quad (6.2)$$

in which σ is the shear stress and $\dot{\epsilon}$ represents the rate of shear or the shear gradient. The proportionality constant in Eq. (6.2) is the viscosity, which is a material constant for simple liquids.

Before proceeding, some definitions are useful. Stress is the ratio of the force on a body to the cross-sectional area of the body. The true stress refers to the infinitesimal force per (instantaneous) area, while the engineering stress is the force per initial area. Strain is a measure of the extent of the deformation. Normal strains change the dimensions, whereas shear strains change the angle between two initially perpendicular lines. In correspondence with the true stress, the Cauchy (or Euler) strain is measured with respect to the deformed state, while the Green's (or Lagrange) strain is with respect to the undeformed state.

The simple form of Eqs. (6.1) and (6.2) embodies two assumptions. The material is isotropic, so that the properties are the same in all directions. More generally, the stress is a tensor

$$\sigma_{ij} = \begin{pmatrix} \sigma_{11} & \sigma_{12} & \sigma_{13} \\ \sigma_{21} & \sigma_{22} & \sigma_{23} \\ \sigma_{31} & \sigma_{32} & \sigma_{33} \end{pmatrix} \quad (6.3)$$

in which the subscripts refer to the rectilinear coordinates. To avoid rotation or translation of a body, $\sigma_{12} = \sigma_{21}$, $\sigma_{13} = \sigma_{31}$, and so on; thus, only six of the stress components are unique. The set of axes for which one of the normal stresses is maximum defines the principal stresses

$$\sigma_{ij} = \begin{pmatrix} \sigma_{11} & 0 & 0 \\ 0 & \sigma_{22} & 0 \\ 0 & 0 & \sigma_{33} \end{pmatrix}. \quad (6.4)$$

These can be found as roots of the equation

$$\sigma^3 - I_1\sigma^2 - I_2\sigma - I_3 = 0 \quad (6.5)$$

in which I_1 , I_2 , and I_3 are the so-called strain invariants,

$$I_1 = \lambda_1^2 + \lambda_2^2 + \lambda_3^2, \quad I_2 = \lambda_1^2\lambda_2^2 + \lambda_1^2\lambda_3^2 + \lambda_2^2\lambda_3^2, \quad I_3 = \lambda_1^2\lambda_2^2\lambda_3^2. \quad (6.6)$$

Strain invariants are independent of the axes used to define the geometry, enabling calculations for inhomogeneous deformations without explicit consideration of the principal directions. During a homogenous deformation,

TABLE 6.1 Common Elastic Constants and Their Interrelationships (Mott and Roland, 2009)

Elastic Constant	Definition	Relation to Poisson's Ratio
$E \equiv$ Young's modulus	$\varepsilon = \varepsilon_{11}; \varepsilon_{22} = \varepsilon_{33} = -\nu\varepsilon_{11};$ other $\varepsilon_{ij} = 0$	—————
$G \equiv$ shear modulus	$\varepsilon = \varepsilon_{12};$ other $\varepsilon_{ij} = 0; \gamma_{12}$ $= \varepsilon_{12} + \varepsilon_{21} = 2\varepsilon_{12}$	$\nu = \frac{E}{2G} - 1$
$B \equiv$ bulk modulus	$\varepsilon = \varepsilon_{11} = \varepsilon_{22} = \varepsilon_{33};$ other $\varepsilon_{ij} = 0$	$\nu = \frac{1}{2} - \frac{E}{6B}$
$M \equiv$ longitudinal modulus	$\varepsilon = \varepsilon_{11};$ other $\varepsilon_{ij} = 0$	$\nu = \frac{1}{4} \left[\frac{E}{M} - 1 \pm \left(\frac{E^2}{M^2} - 10 \frac{E}{M} + 9 \right)^{1/2} \right]$
$E \equiv$ biaxial modulus	$\sigma = \sigma_{11} = \sigma_{22};$ other $\sigma_{ij} = 0$	$\nu = 1 - \frac{E}{H}$

parallel lines remain parallel, whereas inhomogeneous (heterogeneous) strains are nonuniform and irregular, distorting the body into a more complex form. Most mathematical treatments assume that strains are homogeneous.

For an isotropic body, there are only two stress components that are independent of the other. This means that while different loadings and strains can be imposed, the material constants relating stress and strain are not all unique. There are six common elastic constants (Table 6.1), including Poisson's ratio, defined as the ratio of the lateral strain accompanying a longitudinal strain, $\nu = -\varepsilon_{22}/\varepsilon_{11}$. Since only two are unique for an isotropic body, each elastic constant can be expressed as a function of any other pair; these expressions are tabulated in Table 6.1 in terms of Poisson's ratio (Mott and Roland, 2009).

The second assumption implicit in Eqs. (6.1) and (6.2) is that the material is homogeneous, meaning its properties are the same at all points. (This differs from the idea of a homogeneous, or affine, strain, in which the displacements at all points are linear functions of their original coordinates.) Of course, because of their molecular structure, no material is strictly homogeneous. Continuum mechanics is always an approximation to real materials, with homogeneity being relevant to the type of measurement under consideration. For example, rubber reinforced with filler is homogeneous on the scale of a bulk mechanical measurement, notwithstanding the marked difference in properties between the polymer and the rigid particles, which have dimension on the order of 10–100 nm.

The defining characteristic of rubbery polymers is their macromolecular size, which can be two orders of magnitude larger than the distance between

atoms. As a result, internal motions occur over a range of length scales, each associated with a different time scale. This means that whether an external perturbation is “slow” or “fast” depends on the mode of motion it excites. Invariably, some modes move on the time scale of the perturbation, dissipating energy and causing a peak in the out-of-phase, or loss, component of the dynamic response, at a frequency equal to that of the underlying motion. Other modes, such as vibrations, are relatively fast, responding elastically, or they involve the entire molecule, manifested as flow (in the absence of a network structure). If the time scale of the motion is very long, the mode can be unresponsive to the perturbation; a well-known example is the conformational transitions of a polymer backbone below the glass transition temperature. The net effect of this diversity of modes of motion is a frequency-dependent response to mechanical excitation, or equivalently, a time-varying reaction to a transient perturbation. This means that elastic constants such as E or η are not constant for a viscoelastic material, but vary with dynamic frequency or time.

Although the rheology and processing of rubber entails mechanical properties as described earlier, viscoelasticity encompasses other manifestations of the same underlying motions, such as dielectric polarization, dynamic birefringence, and the inelastic scattering of light, X-rays, and neutrons. Viscoelastic materials exhibit a second, related property, the simultaneous storage and dissipation of energy, from which the term originates. The normal forces accompanying shear flow of polymers are due to the elasticity of the material, and hence another manifestation of viscoelasticity.

Viscoelasticity can also be observed in nonpolymeric materials, although usually only over a limited range of conditions (whereas polymers have rate-dependent mechanical properties at almost all temperatures). An example is the viscosity of supercooled molecular liquids (Angell et al., 2000; Roland et al., 2005). Creep of metals under sustained loading at elevated temperature is referred to as viscoelasticity (Kennedy, 1953; McLean, 1966), although the behavior is caused by changes in dislocations or grain size. Strictly speaking, viscoelasticity refers only to the properties of an unchanging material; if the variation in the response with time is due to changes of the material itself (e.g., the drying of concrete or chain scission in a sheared polymer), this is not viscoelasticity.

6.2 LINEAR VISCOELASTICITY

6.2.1 Material Constants

Due to their viscoelastic nature, the response of polymers depends entirely on the loading history, and the simple inverse relationship between moduli and compliances is lost. Thus, Eq. (6.1) for application of a shear strain becomes

$$G(t) = \sigma(t)/\varepsilon_0 \quad (6.7)$$

in which $G(t)$ is the stress relaxation modulus; tensile stresses would yield the corresponding tensile relaxation modulus, $E(t)$. Imposing a constant load yields the compliance, which for shear is

$$J(t) = \gamma(t)/\sigma_0. \quad (6.8)$$

The two response functions are related as

$$\int_0^t G(u)J(t-u)du = t \quad (6.9)$$

but the stress relaxation and compliance are not reciprocals

$$G(t)J(t) < 1. \quad (6.10)$$

For a viscoelastic material, the viscosity in the limit of zero-shear rate, the Newtonian viscosity, can be obtained from the integral of the stress relaxation modulus

$$\eta_0 = \int_0^\infty G(t)dt = \int_0^\infty tG(t)d \ln t. \quad (6.11)$$

A logarithmic time axis is necessary because of the very broad time scale of the dynamics of polymers.

The steady-state recoverable compliance, which is a measure of the elastic strain, can be calculated using

$$J_s^0 = \int_0^\infty tG(t)dt \bigg/ \left(\int_0^\infty G(t)dt \right)^2. \quad (6.12)$$

The compliance function measured in a creep experiment can be decomposed into recoverable and viscous flow components

$$J(t) = J_r(t) + t/\eta, \quad (6.13)$$

where $J_r(t)$ is the recoverable compliance. After steady state is attained, and the viscosity becomes equal to η_0 ,

$$J_s^0 = \lim_{t \rightarrow \infty} J_r(t). \quad (6.14)$$

The steady-state recoverable compliance can be measured by fitting Eq. (6.13) to creep data at long times, or more accurately, J_s^0 is determined from the recovery after removal of the stress subsequent to attainment of steady-state flow.

The Kramers-Kronig formula relates the stress relaxation modulus to dynamic quantities (Kronig, 1926; Kramers, 1927)

$$\int_0^\infty G'(\omega) \frac{\sin \omega t}{\omega} d\omega = \int_0^\infty G''(\omega) \frac{\cos \omega t}{\omega} d\omega = \frac{\pi}{2} G(t) \quad (6.15)$$

or the inverse relations for the storage modulus

$$G'(\omega) = \omega \int_0^{\infty} G(t) \sin(\omega t) dt \quad (6.16)$$

and the loss modulus

$$G''(\omega) = \omega \int_0^{\infty} G(t) \cos(\omega t) dt. \quad (6.17)$$

An approximate relation is (Tschoegl, 1989)

$$G''(\omega) \approx \frac{\pi}{2} \frac{dG'(\omega)}{d \ln \omega}. \quad (6.18)$$

An analogous expression for the dielectric loss in terms of the derivative of the permittivity is commonly used to avoid the problem of dielectric loss peaks being masked by dc conductivity (the latter not contributing to the in-phase response) (Wubbenhorst and Van Turnhout, 2002).

The dynamic viscosity, $\eta = G''(\omega)/\omega$, yields the terminal viscosity in the limit of zero frequency

$$\eta_0 = \lim_{\omega \rightarrow 0} G''(\omega)/\omega \quad (6.19)$$

and J_s^0 can be obtained from the zero-shear-rate limiting value of the storage modulus

$$J_s^0 = \eta_0^{-2} \lim_{\omega \rightarrow 0} \omega^{-2} G'(\omega). \quad (6.20)$$

Alternatively, from steady shearing experiments, which yield η_0 directly in the limit of low shear rate, the steady-state recoverable compliance can be obtained from the first normal stress coefficient, Ψ_0 , which is the ratio of the first normal stress difference to the square of the shear rate, measured at low shear rate

$$J_s^0 = \frac{\Psi_0}{2\eta_0^2}. \quad (6.21)$$

From Eq. (6.12) the steady-state recoverable compliance is also given by

$$J_s^0 = \eta_0^{-2} \int_0^{\infty} t G(t) dt. \quad (6.22)$$

It follows from Eqs. (6.11) and (6.17) that

$$\eta_0 = \lim_{\omega \rightarrow 0} G''(\omega)/\omega \quad (6.23)$$

Experimentally steady state in a transient experiment implies

$$J(t) \sim t. \quad (6.24)$$

The steady-state recoverable compliance is an important rheological parameter because it is very sensitive to the high molecular tail of the molecular weight distribution, and thus can be correlated with elastic properties of a rubber.

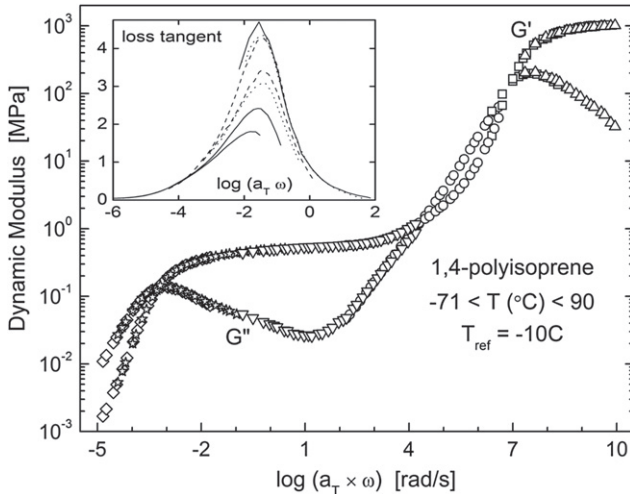


FIGURE 6.2 Dynamic shear modulus master curve for 1,4-polyisoprene. Although the time-temperature shifting is apparently satisfactory, there is a breakdown in the glass transition zone, as seen in the inset, showing the changing shape of the loss tangent peak for different temperatures (Santangelo and Roland, 1998).

The defining feature of the dynamics of rubber comes from the entanglement of the chains, due to their uncrossability. These entanglements are topological and entirely intermolecular, since the volume of a given chain is pervaded by many other chains. Due to entanglements, there is a range of frequencies over which the storage modulus (or equivalently, the relaxation modulus versus time) has a nearly constant magnitude, G_N . This rubbery plateau is evident in the dynamic mechanical spectra for polyisoprene in Figure 6.2 (Santangelo and Roland, 1998). The entanglements cause chain motion to be anisotropic, favoring the chain direction (de Gennes, 1979), and are described by the tube model of Doi and Edwards (1986). The model has two species-dependent parameters, the Rouse friction coefficient, ζ , and a parameter characterizing the concentration of entanglements. From Eq. (6.15) (Kronig, 1926; Kramers, 1927),

$$G_N = \frac{2}{\pi} \int_{-\infty}^{+\infty} G''(\omega) d \ln \omega. \quad (6.25)$$

The upper limit in Eq. (6.25) is imposed empirically to avoid inclusion of the glass transition zone. When the material is plasticized with diluent, G_N decreases by roughly the square of the polymer volume fraction.

A determination of how G_N depends on the chemical structure of a polymer requires a definition of an entanglement. Various ideas have been proposed: a fixed number of binary contacts per entanglement (Brochard and De Gennes, 1977) or per entanglement volume (Colby et al., 1992); a fixed number of strands per entanglement volume (Ronca, 1983; Lin, 1987; Kavassalis and

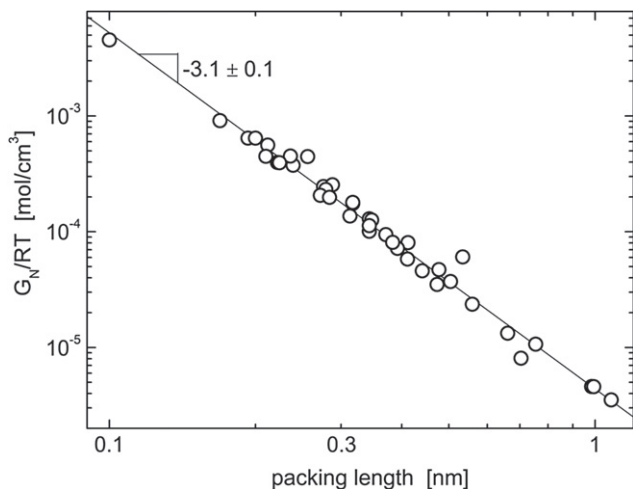


FIGURE 6.3 Entanglement interaction density, defined as the ratio of the plateau modulus to the thermal energy, versus the packing length for different polymers. The power-law slope is indicated (Roland, 2011; Everaers et al., 2004).

Noolandi, 1989; Fetters et al., 1999); or some fraction of the number of interchain contacts (Graessley and Edwards, 1981; Heymans, 2000; Fetters et al., 1994, 2002; Richter et al., 1993). Analysis of experimental data leads to the rough estimate that six binary contacts are necessary to produce one entanglement (Graessley, 2008). The greater the volume pervaded by a chain, the more it encounters neighboring chains; thus, stiffer polymer backbones having smaller, less bulky repeat units are expected to be more entangled. In Figure 6.3 (Roland, 2011; Everaers et al., 2004) the plateau modulus of various polymers is plotted versus the packing length, $l_p \equiv \frac{M}{\rho N_A \langle R_g^2 \rangle}$, in which $\langle R_g^2 \rangle$ is the mean square radius of gyration, ρ is the mass density, and N_A is Avogadro's number. The packing length is the ratio of the volume of a chain to the square of its radius. The data in Figure 6.3 indicate that G_N is inversely proportional to the cube of l_p .

A characteristic relaxation time for a rubber can be defined from the ratio of the zero-shear viscosity and the plateau modulus (Roland, 2011; Ferry, 1980)

$$\tau_0 = \eta_0 G_N. \quad (6.26)$$

τ_0 is a terminal relaxation time describing chain motions. Other global relaxation times can be defined experimentally, for example as the inverse of the frequency of the maximum in the terminal dispersion in the loss modulus, τ_{\max} ; from the time for equilibration following cessation of nonlinear shear flow, $\tau_{R,\eta}$, measured by recovery of the overshoot in the transient viscosity; the corresponding time for recovery of the overshoot in the second normal

TABLE 6.2 Comparison of Global Relaxation and Recovery Times for Entangled 1,4-Polybutadiene Solutions (Roland and Robertson, 2006)

Relaxation Time	$\varphi M_w / M_e^a$	
	30	47
$\log \tau_0$	-0.64 ± 0.03	-0.10 ± 0.03
$\log \tau_{\max}$	-1.49 ± 0.01	-0.944 ± 0.03
$\log \tau_{R,\eta}$	0.84 ± 0.02	1.68 ± 0.02
$\log \tau_{R,G}$	1.59 ± 0.05	1.96 ± 0.05
$\log \tau_{R,\Psi}$	0.53 ± 1	0.93 ± 0.54

^aNumber of entanglements per chain.

stress coefficient, $\tau_{R,\Psi}$; and $\tau_{R,G}$, the time for the dynamic storage modulus to return to its equilibrium value after nonlinear flow. Table 6.2 (Roland and Robertson, 2006) compares these different relaxation times for high molecular weight 1,4-polybutadiene. Their magnitudes differ by as much as three orders of magnitude. It has also been found that the temperature dependence of these various relaxation times can be different (Roland et al., 2004).

6.2.2 Boltzmann Superposition Principle

If the rubber exhibits linear mechanical behavior, defined by proportionality between stress and strain and time invariance of the response, the Boltzmann superposition equation can be used to predict the stress for any strain history (Boltzmann, 1874; Larson, 1988). In terms of the shear relaxation modulus, the equation is

$$\sigma(t) = \int_0^t G(t-u) \frac{d\varepsilon}{du} du. \quad (6.27)$$

Rewriting Eq. (6.27) to make explicit the additivity of the stresses

$$\sigma(t) = \int_0^t \frac{dG(t-u)}{du} (\varepsilon(t) - \varepsilon(u)) du + G(t)\varepsilon(t). \quad (6.28)$$

In this equation $\frac{dG(t-u)}{du} du$ represents the “fading memory”; that is, the survival probability at time t of a stress created at time u .

While all polymers obey Eq. (6.27) at sufficiently small strains, for rubbers this linear behavior extends over a very wide range (Yannas, 1974; Chang et al., 1976). When the strains are too large for a linear response, Bernstein (1963, 1964) and, independently, Kaye (1962) developed an integral constitutive

equation to describe the nonlinear viscoelastic properties, known as the K-BKZ equation

$$\sigma(t) = \int_0^t [G(t-u, \varepsilon(t-u))] \frac{d\varepsilon}{du} du. \tag{6.29}$$

If the relaxation behavior, $G(t)$, in Eq. (6.29) is independent of strain, the behavior is referred to as “time invariant.” This decoupling of time and strain effects leads to a simpler expression

$$\sigma(t) = \int_0^t [G(t-u)g(\varepsilon)] \frac{d\varepsilon}{du} du. \tag{6.30}$$

The damping function, $g(\varepsilon)$, in Eq. (6.30) accounts for lack of proportionality between stress and strain. The product, $g(\varepsilon)\varepsilon$, quantifies the nonlinear elasticity ($g(\varepsilon) = 1$ for linear viscoelastic behavior). Separability of time and strain is illustrated for 1,4-polyisoprene in Figures 6.4 and 6.5; the time-dependence of the stress relaxation is the same for shear strains of varying amplitude and for different modes of deformation (Fuller, 1988).

Absent mechanisms such as strain crystallization or the finite extension of the chains, uncrosslinked rubbers usually strain-soften, which means that $g(\varepsilon)$ decreases with strain. A damping function that has been shown to successfully describe elastomers for tensile strains of a few hundred percent is (Roland, 1989)

$$g(\varepsilon) = \left(1 + \frac{c_2}{c_1} \lambda^{-1} \right), \tag{6.31}$$

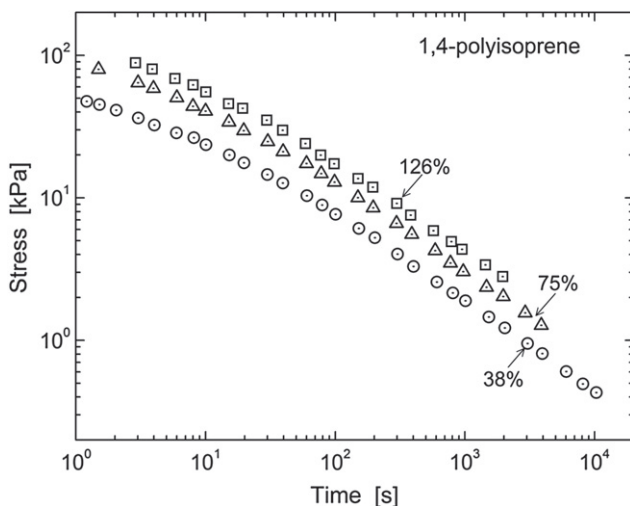


FIGURE 6.4 Stress relaxation of synthetic 1,4-polyisoprene at the indicated shear strains. The parallel nature of the curves reflects the invariance of the time-dependence to strain (Fuller, 1988).

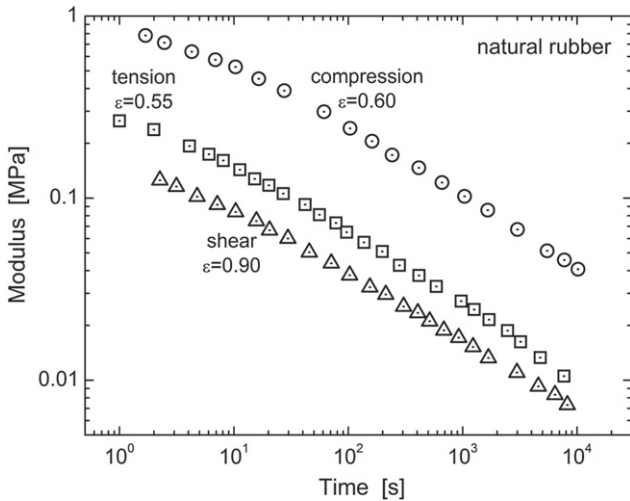


FIGURE 6.5 Stress relaxation modulus of natural rubber at different types and magnitudes of strain. The curves are approximately parallel, indicating that strain and time effects are decoupled (Fuller, 1988).

where c_1 and c_2 are material constants. For a single-step strain, Eq. (6.29) simplifies to

$$\sigma(\varepsilon, t) = G(t)g(\varepsilon)\varepsilon. \quad (6.32)$$

For continuous straining the integral in Eq. (6.30) can be approximated as a series of step strains, each described by Eq. (6.32). From these equations the stress for arbitrary strain history can be predicted, although the calculation requires that both the stress relaxation function and the strain-dependence of the modulus be determined in separate experiments. This general approach to predicting the rheology of polymer melts has met with good success (Tanner, 1988).

The accuracy of K-BKZ predictions can be improved with the addition of correction terms to account for other mechanisms (Vrentas et al., 1991; Coleman and Zapas, 1989; McKenna and Zapas, 1979). Introducing the “independent alignment approximation” to the Doi-Edwards tube model of polymer dynamics yields the K-BKZ form (Doi, 1980). (This independent alignment approximation assumes the relative position of every segment does not change following straining; that is, the “tube” of entanglement constraints does not retract.) The Doi-Edwards damping function for shear can be approximated as

$$g(\varepsilon) = \left(1 + \frac{\zeta}{3}\varepsilon^2\right)^{-1}, \quad (6.33)$$

where ζ is a parameter fitted to experimental data (Larson, 1985; Larson and Valesano, 1986). Using $\zeta = 0.43$ gives results corresponding to the tube model with constraint release. Constraint release refers to diffusion of the segments comprising the tube of entanglements, whereas in the original tube model, strictly applicable only to a chain dissolved in a network, the segments of the tube are fixed (Milner, 1996).

6.2.3 Time-Temperature Equivalence

Most mechanical test instruments have a limited dynamic range, typically down to ca. 10^{-4} s^{-1} for low strain rates, which almost always requires transient measurements, and up to about 100 s^{-1} on the high frequency end, usually employing dynamic measurements. Servohydraulic test systems can achieve higher speeds, but with limitations on the attainable strains (Bergstrom and Boyce, 1998; Arruda et al., 2001). If only the linear viscoelastic response is to be measured, dielectric spectroscopy (Kremer and Schonhals, 2003; McCrum et al., 1967) can be used. Dielectric spectroscopy can be carried out routinely over 11 decades of frequency, extending to GHz; this range can be extended to as much as 18 decades (Schneider et al., 1999), although this requires corrections be made for effects from the connectors and cables. However, dielectric relaxation only probes the local segmental dynamics of polymers, except for the few cases in which a dipole moment is present parallel to the polymer chain. For the latter the chain modes are dielectrically active, and the dynamics of the chain end-to-end vector can be measured. Although dielectric relaxation times are smaller than the corresponding mechanical relaxations, their respective dependences on temperature (Boese et al., 1989; Colmenero et al., 1991, 1994; Paluch et al., 2002, 2003) and pressure (Bair and Winer, 1980; Roland et al., 2006) are the same. Another advantage of dielectric spectroscopy is the relative ease of obtaining measurements at elevated hydrostatic pressure (Roland et al., 2005; Skorodumov and Godovskii, 1993; Floudas, 2003). Few mechanical studies of the effect of pressure have been carried out, and these are usually limited to studying the viscosity of low molecular weight polymers (Hellwege et al., 1967; Fillers and Tschoegl, 1977; Bair, 2002). The dynamic modulus of polymer melts can be measured in a rheometer pressurized with a gas (Han and Ma, 1983; Gerhardt et al., 1997; Royer et al., 2000), but since gases dissolve in the material, the consequent plasticization can introduce error.

(i) Superposition Principle

The most common means to extend the frequency scale is to invoke time-temperature superpositioning (Ferry, 1980). If all motions of a polymer contributing to a particular viscoelastic response are affected the same by temperature, then changes in temperature only alter the overall time scale; such a material is thermorheologically simple. Thermorheological simplicity means conformance to the time-temperature superposition principle, whereby lower and higher strain rate data can be obtained from measurements at higher and lower temperatures, respectively.

Time-temperature superpositioning was originally derived from free volume models, which assume that the rates of molecular motions are governed by the available unoccupied space. Early studies of molecular liquids led to the Doolittle equation, relating the viscosity to the fractional free volume, $f(\equiv V/(V - V_0))$, where V is the specific volume and V_0 is the occupied volume normalized by the mass) (Doolittle and Doolittle, 1957; Cohen and Turnbull,

1959):

$$\log \eta(T) = \log A_D + B_D/f(T), \quad (6.34)$$

with A_D and B_D constants. However, Eq. (6.34) only approximately fits experimental data (Corezzi et al., 1999; Paluch, 2001; Schug et al., 1998). The assumption that the free volume expands linearly with temperature, $\left. \frac{df}{dT} \right|_p \sim T$, leads to the Williams-Landel-Ferry (WLF) equation (Ferry, 1980; Williams et al., 1955):

$$\log a(T) = \log a(T_R) - \frac{c_1(T - T_R)}{c_2 + T - T_R}, \quad (6.35)$$

where T_R is an arbitrary reference temperature. Assuming the WLF constants c_1 and c_2 are functions of the free volume leads to “universal values” of $c_1 = 8.86$ and $c_2 = 101.6$ (Williams et al., 1955). In Eq. (6.35) $a(T)$ is a time-temperature shift factor, defined for the viscosity as $a(T) = \eta(T)/\eta(T_R)$, or for the relaxation times as $a(T) = \tau(T)/\tau(T_R)$. (η and τ are proportional except near the glass transition (Chang and Sillescu, 1997; Rössler, 1990; Fischer et al., 1992); cf. Eq. (6.26).) Shift factors are used because the actual magnitude of the viscoelastic quantities does not affect $t - T$ superpositioning, only their change with temperature. An ostensibly different, but mathematically equivalent expression to Eq. (6.35) is due to Vogel, Fulcher, Tamman, and Hesse (Ferry, 1980):

$$\log \tau(T) = \log \tau_\infty + \frac{b_{\text{VFTH}}}{T - T_V}, \quad (6.36)$$

in which $b_{\text{VFTH}} (=c_1/c_2)$, $T_V (=T_R - c_2)$, and τ_∞ are constants (Zallen, 1981). At the Vogel temperature, T_V , the dynamics would diverge if not for intervention of the glass transition. T_V is often taken to be the Kauzmann temperature at which the extrapolated liquid entropy equals the crystal entropy, ostensibly in violation of the third law of thermodynamics (“Kauzmann paradox”) (Angell, 1991).

Cohen and Grest (1979, 1984) and Grest and Cohen (1981) derived a more rigorous free volume model, in which molecules have mobility only when local continuity of empty space exists. Generally free volume models have fallen into disfavor, due to the unphysical results they lead to; for example, free volumes can become negative (Williams and Angell, 1977) or change less with pressure than the occupied volume (Ferry, 1980). Nevertheless, Eqs. (6.35) or (6.36) can still be used to fit experimental data. However, the absence of a firm theoretical foundation means that the validity of time-temperature superpositioning must be established empirically for any material. A major development in the study of polymer viscoelasticity was in 1949, when samples of a high molecular weight polyisobutylene were distributed to laboratories around the world. Both transient, in particular stress relaxation measurements (Andrews and Tobolsky, 1951), and dynamic experiments (Fitzgerald et al., 1953; Ferry et al., 1953) were carried out, with the data spanning 15 decades of frequency. The successful

superpositioning of these results led to the acceptance of time-temperature superpositioning as a method of converting viscoelastic data for polymers obtained over a narrow dynamic range to master curves covering many decades of reduced time or frequency (Roland, 2011; Ferry, 1980; Marvin, 1953).

The four requirements for thermorheological simplicity are:

- The local friction coefficient is the same for all motions underlying the viscoelastic property of interest.
- The polymer does not degrade, crystallize, physically age, or undergo other changes over the course of the measurements.
- At high strain rates, the deformation period is not less than the time required for stress waves to travel through the material; this ensures spatial uniformity of the stress.
- Heat build-up, more pronounced for low temperatures and high rates, causes no deviation from isothermal conditions.

A typical master curve is shown in Figure 6.2 (Santangelo and Roland, 1998) for dynamic shear data of a high molecular weight 1,4-polyisoprene measured over about a 160° range, yielding 15 decades of reduced frequency (the actual data spanned less than 5 decades). A tensile stress relaxation master curve for a polyurea rubber that spans 13 decades is displayed in Figure 6.6 (Knauss and Zhao, 2007).

Although time-temperature superpositioning can be very useful, in the glass transition (softening) zone of the viscoelastic response, polymers are thermorheologically complex. This breakdown of time-temperature superpositioning is caused by the weaker temperature dependence of the chain dynamics

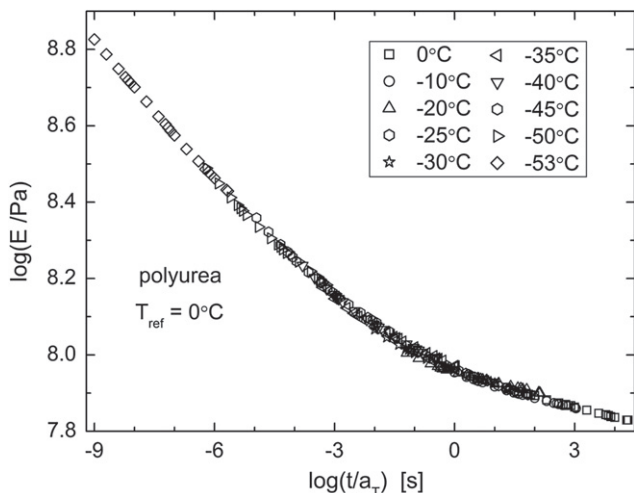


FIGURE 6.6 Tensile stress relaxation modulus of an elastomeric polyurea. Similar to the data in Figure 6.2, there is a breakdown of the time-temperature superpositioning in the glass transition zone (Knauss and Zhao, 2007).

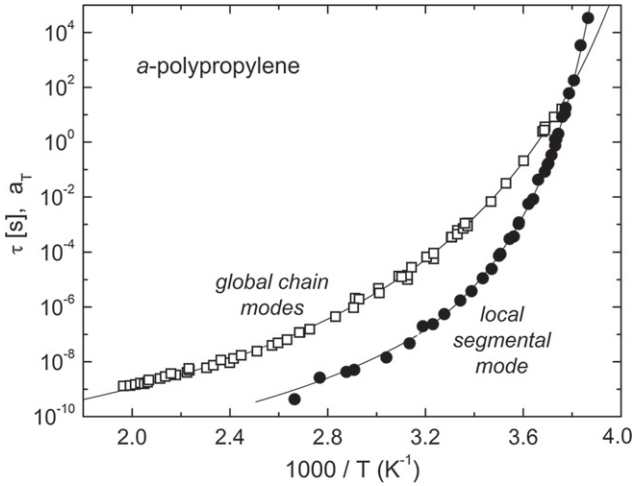


FIGURE 6.7 Atactic polypropylene segmental relaxation times (solid symbols) from mechanical spectroscopy, dynamic light scattering, dielectric relaxation, and ^{13}C NMR, along with the global time-temperature shift factors (open symbols) from dynamic mechanical spectroscopy, creep compliance, and viscosity. Vertical shifts were applied to superpose the data (Roland et al., 2001).

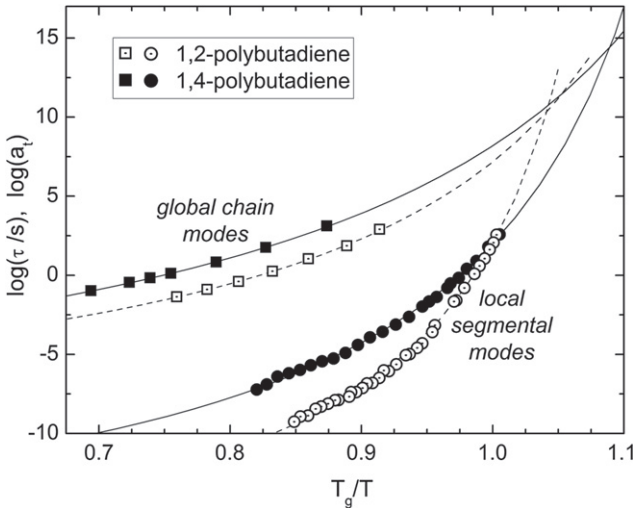


FIGURE 6.8 Local segmental relaxation times (circles) and terminal shift factors (squares) for polybutadienes. The fitted VFTH equations illustrate the marked differences in temperature-dependence of the local and global dynamics (Robertson and Rademacher, 2004).

in comparison to the local segmental modes. Well above the glass transition, relaxation times (or shift factors) for the chain and segmental dynamics are proportional, as shown in Figure 6.7 for *atactic* polypropylene (Roland et al., 2001) and in Figure 6.8 for polybutadiene (Robertson and Rademacher, 2004).

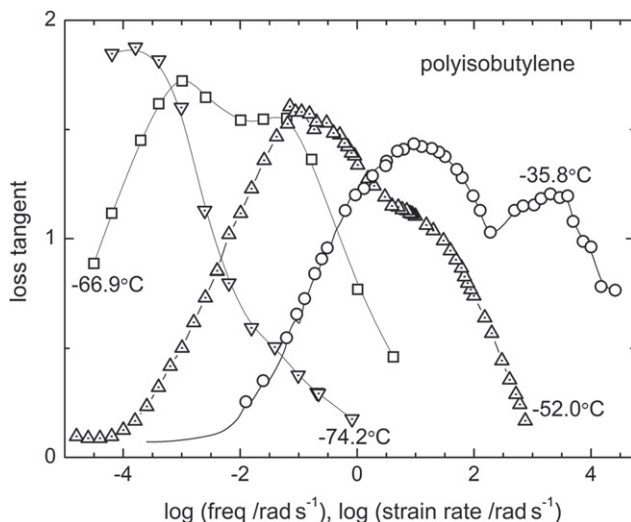


FIGURE 6.9 Loss tangent of polyisobutylene measured by dynamic mechanical spectroscopy and calculated from the recoverable creep compliance. These are not master curves; the abscissa is the actual frequency (Plazek et al., 1995).

However, for measurements within the glass transition zone, where both the chain and the segmental modes contribute, the viscoelastic data do not time-temperature superpose accurately. This breakdown of the time-temperature superpositioning was first discovered for polystyrene (Plazek, 1965) and has since been observed for every polymer for which sufficient data exist (Plazek, 1996; Ngai et al., 1995). Examples of thermorheological complexity include polyisobutylene (Figure 6.9) (Plazek et al., 1995), polyvinylacetate (Plazek, 1980), polypropylene glycol (Ngai et al., 1992), poly(phenylmethylsiloxane) (Plazek et al., 1994), polybutadiene (Robertson and Rademacher, 2004; Palade et al., 1995), atactic polypropylene (Santangelo et al., 1996), poly(alkyl glycidyl ether) (Yamane et al., 2005), polymethylmethacrylate (Plazek et al., 1988), and both the polyisoprene in Figure 6.2 (Santangelo and Roland, 1998) (see inset to figure) and the polyurea in Figure 6.6 (Pathak et al., 2008). The important point when utilizing $t - T$ superpositioning is that high temperature measurements of chain (terminal) properties cannot be combined with low temperature measurements of segmental relaxation times, because the extrapolation of the combined shift factors will be subject to very large errors. This is evident in the crossing of the fits to Eq. (6.36) for the local and global dynamics for the polybutadienes in Figure 6.8.

(ii) Density Scaling

A more realistic alternative to free-volume-derived models is to interpret relaxation and related properties of polymers in terms of the interactions among segments. Thus, in the softening regime of the viscoelastic spectrum, falling

intermediate to the rubbery and glassy plateaus, the polymer dynamics entails jumps over potential barriers that are large compared to the available thermal energy (Goldstein, 1969; Stillinger and Weber, 1984; Sampoli et al., 2003). The dense packing at lower temperatures, however, means that the segmental dynamics are correlated—motion of a given segment occurs in cooperative fashion with neighboring segments. This interpretation of the dynamics requires consideration of the nature of the intermolecular potential governing these reciprocal interactions among segments. A simplified potential that considers only two-body interactions is the symmetric Lennard-Jones (LJ) potential energy function

$$U(r) = 4\hat{\epsilon} \left[(r_0/r)^{12} - (r_0/r)^6 \right], \quad (6.37)$$

where $\hat{\epsilon}$ is a measure of the depth of the potential well and r the separation between segments (which are taken to be spherical particles of radius r_0). The attractive term in this equation has an exponent equal to six because only van der Waals dispersion interactions are considered. The repulsive forces have a stronger dependence on particle separation than the attractive forces; moreover, unlike van der Waals forces, the distance dependence varies with chemical structure (Moelwyn-Hughes, 1961; Bardik and Sysoev, 1998). A more realistic form of the LJ function is then

$$U(r) = 4\hat{\epsilon} \left[(r_0/r)^m - (r_0/r)^6 \right], \quad (6.38)$$

where the value of m depends on the species.

If the primary focus is on the segmental dynamics and properties involving local interactions, the attractive forces can be ignored, since they are long ranged and tend to cancel locally (Widen, 1967; Chandler et al., 1983; Stillinger et al., 2001). This follows from the fact that the force on a segment is the vector sum of all forces from neighboring segments, and there are many such neighbors (Widom, 1999). Thus, an approximate form for the potential can be assumed (Hansen, 1970; March and Tosi, 2002):

$$U(r) = \hat{\epsilon}(r_0/r)^m. \quad (6.39)$$

This inverse power law (IPL) neglects attractive forces, consistent with the fact that the liquid structure is determined primarily by packing effects, which depend only on the repulsions (Hoover and Ross, 1971; Laird and Haymet, 1992). If an IPL accurately represents the local interaction energy between segments, then all thermodynamic properties (such as the energy, volume, and entropy) (March and Tosi, 2002; Hoover and Ross, 1971), as well as dynamic properties (Hiwatari et al., 1974; Ashurst and Hoover, 1975), depend only on the product variable, Tr^m , or in terms of the experimentally measurable specific volume, $V^{m/3}$:

$$\tau = \mathfrak{S} \left(TV^{m/3} \right), \quad (6.40)$$

where \mathfrak{S} is a function. Similar equations can be written for the viscosity, diffusion constant, and so on.

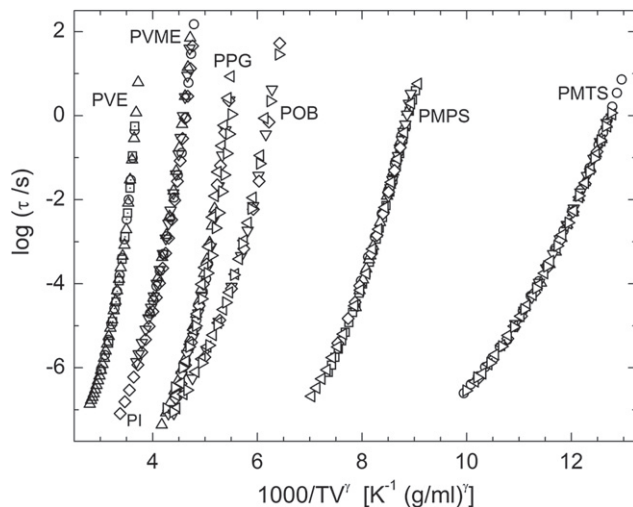


FIGURE 6.10 Density scaling of local segmental relaxation times for polyvinylethylene (PVE, $\gamma = 1.9$); polyvinylmethylether (PVME, $\gamma = 2.55$); polypropylene glycol (PPG, $\gamma = 2.5$); polyoxybutylene (POB, $\gamma = 2.65$); polymethylphenylsiloxane (PMPS, $\gamma = 5.6$); and polymethyl tolylsiloxane (PMTS, $\gamma = 5.0$). For each polymer, every symbol represents a distinct state point, with each symbol type denoting either varying pressure at constant temperature or varying temperature at constant pressure.

The idea is that the polymer dynamics are thermally activated with an activation barrier that depends on volume as $V^{m/3}$. The local segmental relaxation times measured as a function of temperature, pressure, or volume should fall on a single curve when plotted as a function of TV^γ , where the scaling exponent $\gamma = m/3$. Note that if free volume models were exact, $\gamma = \infty$.

Figure 6.10 shows segmental relaxation times for six rubbers measured at different conditions of T and P . For any given polymer, the data collapse to a single dependency on TV^γ . The value of the scaling exponent depends on the material, reflecting differences in the steepness of the intermolecular repulsive potentials. Generally for polymers γ ranges from 1.9 for 1,4-polyisoprene to 5.6 for polymethylphenylsiloxane (Roland et al., 2005). Density scaling has also been applied to viscosity data for polymers (Roland et al., 2006), and to their terminal dispersions (Figure 6.11) (Roland et al., 2004; Casalini and Roland, 2005), although for chain relaxation times the superposition is only approximate (Fragiadakis et al., 2011). In toto, dynamic data for more than 100 polymers and molecular liquids have been shown to conform to density scaling (Roland, 2010, 2011; Fragiadakis and Roland, 2011).

6.2.4 Molecular Weight Dependences

Rheological properties depend strongly on the chain length, but since polymer chains invariably have a distribution of molecular weights, the use of

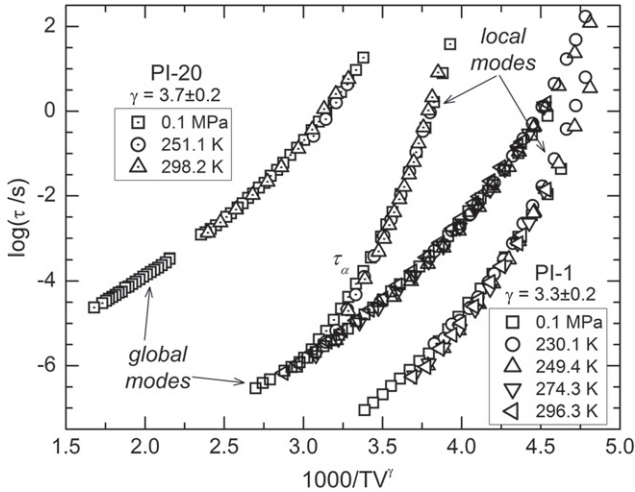


FIGURE 6.11 Density scaling of local segmental and global chain relaxation times for 1,4-polyisoprene having $M_w = 1$ kg/mol (dotted symbols) and 20 kg/mol (open symbols) (Fragiadakis et al., 2011).

averages is required. These include the arithmetic mean or number average molecular weight

$$M_n = \frac{\int_0^{\infty} n(M)M dM}{\int_0^{\infty} n(M) dM}, \quad (6.41)$$

in which n is the number of molecules having molecular weight of M and the weight average molecular weight

$$M_w = \frac{\int_0^{\infty} n(M)M^2 dM}{\int_0^{\infty} n(M)M dM}. \quad (6.42)$$

Higher order moments can be defined, but they are less useful because they cannot be determined as accurately. Other measures of molecular weight include the peak value, M_p , which corresponds to the maximum in the distribution, and M_v , determined from the intrinsic viscosity, $[\eta]$, using the Mark-Houwink relation (Chapter 3 herein):

$$[\eta] = \hat{K} M_v^{\hat{a}}, \quad (6.43)$$

where \hat{K} and \hat{a} are polymer-specific constants. A metric of the breadth of the chain length distribution is the polydispersity index

$$P_i = M_w/M_n. \quad (6.44)$$

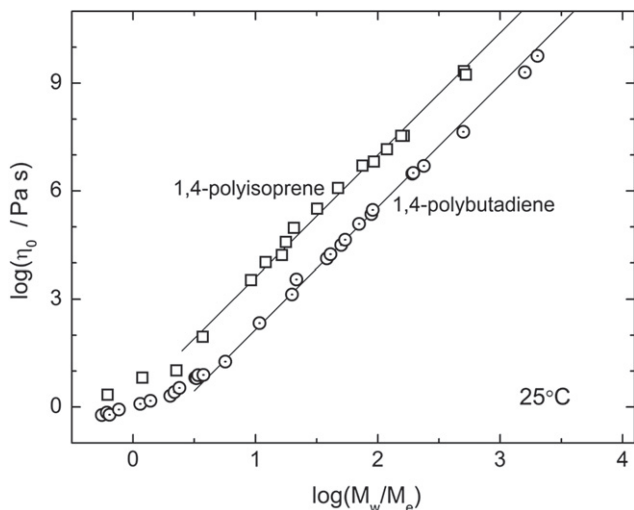


FIGURE 6.12 Terminal viscosity as a function of the molecular weight divided by the entanglement molecular weight; $M_e = 1850$ and 6190 g/mol for 1,4-polybutadiene (circles) and 1,4-polyisoprene (squares), respectively. The solid lines are fits having a slope of 3.4 (Colby et al., 1987; Abdel-Goad et al., 2004).

This index is related to the variance, σ_V^2 , in the chain lengths as

$$\sigma_V^2 = (P_i - 1)M_n^2. \quad (6.45)$$

Most often the average molecular weight is used in relation to rheological properties (Berry and Fox, 1968), although this is only an approximation. When model blends are prepared by mixing monodisperse polymers, the molecular weight dependences are complicated. For example, the melt viscosity is less than the value predicted assuming η is determined by M_w (Watanabe et al., 1995; Monfort et al., 1984; Plazek et al., 1991).

The dependence on molecular weight of most rheological properties becomes much stronger for entangled chains (an exception being J_s^0 , which becomes constant at high M_w (Roland, 2011)). The most commonly reported data are for the melt viscosity, with zero-shear-rate data shown in Figure 6.12 for 1,4-polybutadiene (Colby et al., 1987) and 1,4-polyisoprene (Abdel-Goad et al., 2004). At high molecular weight, the slope of the double logarithmic plot is 3.4, in accord with data for many other materials (Ferry, 1980; Watanabe, 1999; Doi and Edwards, 1986). Interestingly, when compared at equal number of entanglements per chain, η_0 of 1,4-polyisoprene is larger than for the polybutadiene, although when compared at equal M_w , the viscosity of the former is twofold smaller than η_0 of polybutadiene. From Eq. (6.26) the same M_w -dependence is expected for the terminal relaxation time as for η_0 , since J_0 for rubbers is a constant. (Note on cooling toward T_g the recoverable compliance decreases, although the effect can only be observed for low molecular weight polymers

(Roland et al., 2004; Ngai et al., 1995; Santangelo and Roland, 2001).) The diffusion constant of rubbers has a quadratic or somewhat stronger molecular weight dependence (Lodge, 1999; Wang, 2003).

Various characteristic molecular weights can be defined from the molecular weight dependences of the rheological properties, including the molecular weight between entanglements, M_e , determined from the plateau modulus

$$M_e = \frac{\rho RT}{G_N}. \quad (6.46)$$

This equation corresponds to the classic rubber elasticity expression for an affinely deforming network (Roland, 2011). The value of the molecular weight at which the viscosity begins to exhibit a nonlinear dependence is M_c , and since roughly two entanglements are required to affect a chain, there is the approximate relationship, $M_c \sim 2M_e$ (Figure 6.13) (Roland, 2011; Fetters et al., 1999). The molecular weight at which J_s^0 becomes molecular weight invariant is even larger than M_c (Figure 6.14) (Plazek and O'Rourke, 1971; Nemoto et al., 1971, 1972; Roovers, 1985; Roovers and Toporowski, 1990).

The processing of rubber takes place at sufficiently high temperatures that T_g is usually not a relevant parameter, although dynamic properties for different temperatures are often correlated in terms of the difference, $T - T_g$, the ratio T/T_g , or a related quantity (Ferry, 1980; Plazek and Ngai, 1991; Bohmer et al., 1993; Ngai et al., 2008; Ding and Sokolov, 2006). The glass transition defines another characteristic molecular weight, M_∞ , the value at which T_g becomes

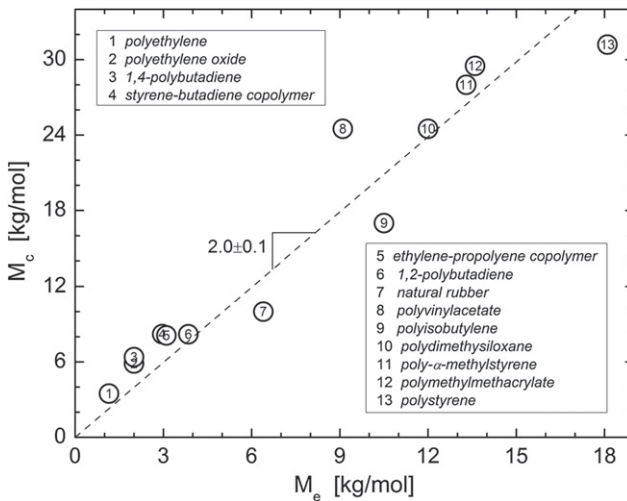


FIGURE 6.13 Characteristic molecular weight at which the viscosity exhibits a change in M -dependence versus the molecular weight between entanglements determined from the plateau modulus (Roland, 2011; Fetters et al., 1999).

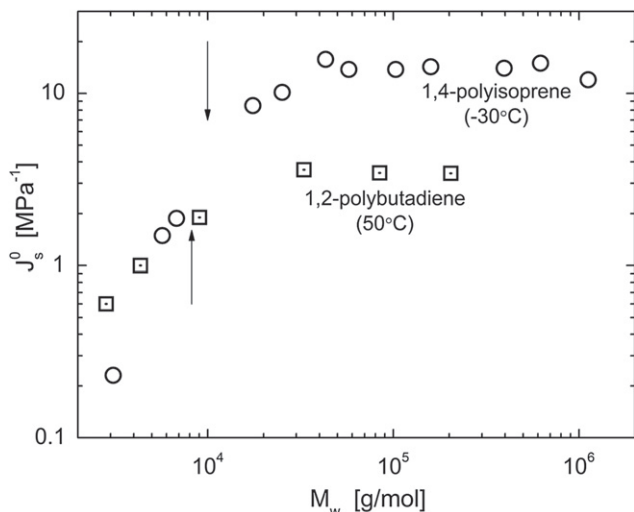


FIGURE 6.14 Steady-state recoverable compliance, which becomes constant at high molecular weight, for 1,4-polyisoprene (circles) and 1,4-polybutadiene (squares). The vertical arrows denote the M_w for entanglements to affect the viscosity, which is smaller than the value of the molecular weight at which J_s^0 become constant (Roland, 2011).

independent of chain length. The general M -dependence of the glass transition can be described empirically (Ueberreiter and Kanig, 1952)

$$T_g = \left(T_{g,\infty}^{-1} + k_{UK}/M_n \right)^{-1}. \quad (6.47)$$

$T_{g,\infty}$ and k_{UK} are material constants, the latter dependent on the chain end groups (Turner, 1978; Danusso et al., 1993). Figure 6.15 shows the fit of Eq. (6.47) to data for 1,4-polybutadiene (Bogoslovov et al., 2010).

6.2.5 Stress Birefringence

An independent method of determining stress, especially useful for materials under flow, is from the optical birefringence. Of course, it is limited to transparent materials, which precludes application to filled polymers. Because of the need for transparency, stress birefringence has been used more often for plastics than rubber. Residual anisotropy due to unrelaxed orientation can also be assessed using birefringence; this is commonly known as the photoelastic effect. Generally the birefringence is directly proportional to the true stress

$$\Delta n = C\sigma, \quad (6.48)$$

where Δn represents the difference in refractive index between the strain direction and transversely, and the stress optical coefficient C is a material constant determined by the chemical structure of the chain repeat unit. This

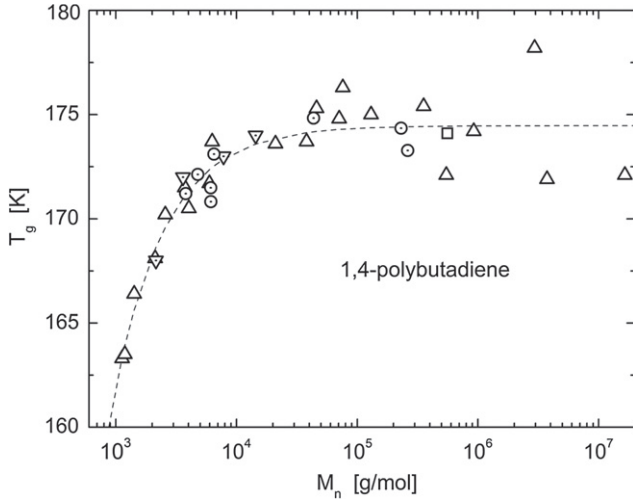


FIGURE 6.15 Glass transition temperatures determined from the thermal expansivity (circles), calorimetry (triangles and squares), Raman scattering (inverted triangles), and as the temperature at which the dielectric relaxation time equals 100 s (star). The solid line is the simultaneous fit of Eq. (6.47) to all data, with the high molecular weight limiting value of $T_{g,\infty} = 174.4$ K (Bogoslovov et al., 2010).

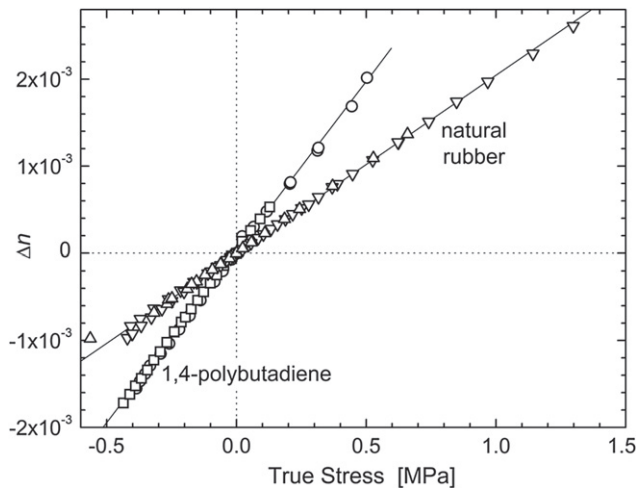


FIGURE 6.16 Optical birefringence for 1,4-polybutadiene and natural rubber networks under tension and compression; the stress optical coefficient is given by the slopes = 3.6 and 2.0 GPa^{-1} , respectively (Mott and Roland, 1996).

stress optical law holds to reasonably high levels of strain, a consequence of the small end-to-end distance of macromolecules compared to their fully extended length. Data for polybutadiene and polyisoprene are shown in Figure 6.16 (Mott

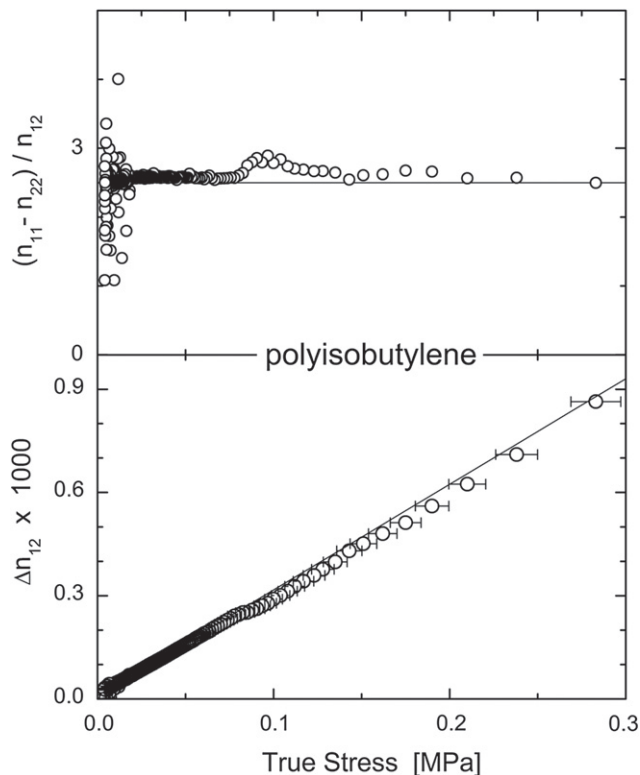


FIGURE 6.17 (Bottom) Birefringence for uncrosslinked PIB after imposition of a shear strain = 2.5. Linear fitting yields 3.07 GPa^{-1} for the stress optical coefficient. (Top) Ratio of refractive index components (1 is the flow direction and 2 the direction of the gradient), which equals the value of the shear strain, in accord with the Lodge-Meissner relation (Eq. (6.66)) (Balasubramanian et al., 2005).

and Roland, 1996). A measure of orientation is the Herman orientation function,

$$f(\theta) = (3\langle \cos^2 \theta \rangle - 1)/2, \quad (6.49)$$

which is equal to the ratio of Δn to the value of the birefringence for complete orientation. In Eq. (6.49) the brackets refer to an average over all chains, with θ the angle between the long axis of the repeat unit and the reference axis. Note that in the liquid crystal literature, $f(\theta)$ is known as the order parameter.

The stress optical law is maintained during relaxation of a deformed rubber (Figure 6.17) (Balasubramanian et al., 2005); moreover, the same proportionality to Δn is maintained for the normal components of the stress. And since orientation of rubber also affects heat conduction (Hands, 1980), there is a corresponding proportionality, known as the “stress-thermal rule,” between stress and the anisotropy of the thermal conductivity (Venerus et al., 1999);

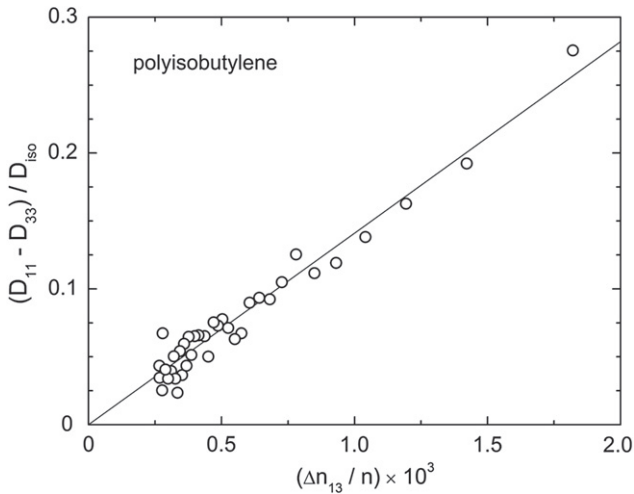


FIGURE 6.18 Normalized difference in thermal diffusivity versus normalized birefringence for polyisobutylene after imposition of a shear strain = 8. The line is the linear fit to the data (Venerus et al., 1999).

consequently, the thermal conductivity is proportional to the birefringence (Figure 6.18) (Balasubramanian et al., 2005; Venerus et al., 1999).

6.3 NONLINEAR VISCOELASTICITY

6.3.1 Shear Thinning Flow

The viscosity of entangled polymers becomes shear-rate dependent when the shear rate exceeds the inverse of the time scale for the terminal dynamics of the chains. This non-Newtonian behavior is a prominent characteristic of rubber, central to processing operations (Figure 6.19). Shear thinning is due to a reversible reduction in the degree of chain entanglement caused by flow (Vinogradov and Belkin, 1965; Simmons, 1968; Tanner and Williams, 1971; Batzer et al., 1980; Isono et al., 1995, 1997; Oberhauser et al., 1998). Since reentanglement of the chains can be slow, the “shear-modified” state of a polymer melt can be exploited to enhance processability of the material. This has been shown to give transient reductions in die swell, for example in polyethylene, polypropylene, and polystyrene melts (Yamaguchi and Gogos, 2001; Rudin and Schreiber, 1983; Leblans and Bastiaansen, 1989; Pohl and Gogos, 1961; Ram and Izrailov, 1986; Kotliar et al., 1990).

Another indication of fewer entanglements is the magnitude of the overshoot in the transient shear stress. For high shear rates, the stress exhibits a maximum, followed by a steady-state value determined by the degree of entanglement under the particular conditions of flow. If the shearing is stopped, the subsequently observed stress overshoot will be smaller. However, its magnitude

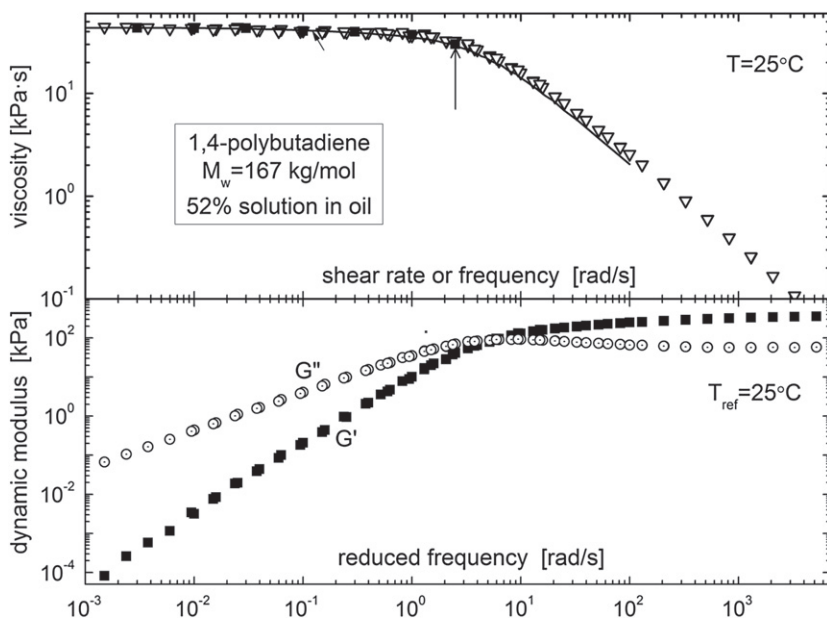


FIGURE 6.19 (Upper panel) Steady-state shear viscosity versus shear rate (solid symbols), dynamic viscosity versus frequency (open symbols), and transient viscosity calculated from Eq. (6.65) versus the inverse of the time of shearing (solid line). (Lower panel) Dynamic storage and loss modulus master curve for the same entangled polybutadiene solution (Roland and Robertson, 2006).

increases with the time prior to restarting the flow, as the chains reentangle (Attane et al., 1985; Dealy and Tsang, 1981; Huppler et al., 1967; Stratton and Butcher, 1973; Menezes and Graessley, 1982; Xu et al., 1995). This effect is illustrated in Figure 6.20 with data for a concentrated polybutadiene solution (Roland and Robertson, 2006; Robertson et al., 2004). The stress overshoot and associated disentanglement requires shear rates in the non-Newtonian regime (Figure 6.21). Note that stress overshoots can occur in any material whose structure is disrupted by flow (Whittle and Dickinson, 1997; DeKee and Fong, 1994), and even in unentangled polymers; however, these effects are usually much weaker (Moore et al., 1999; Santangelo and Roland, 2001) than for entangled polymers. These transient flow phenomena can be described using K-BKZ-type constitutive equations (Eq. (6.29)) (Menezes and Graessley, 1982).

6.3.2 Particulate Fillers

Rubber compounds very often contain small-particle fillers such as carbon black and silica, to improve processability and physical properties, and to reduce material costs. The most common filler is carbon black, use of which as a pigment dates to ca. 4000 BC. Methods to incorporate fillers, and the effect of their distribution and dispersion on properties, are central considerations, with

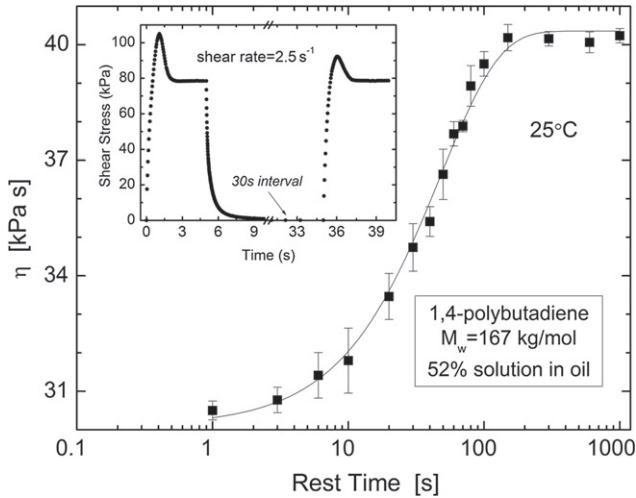


FIGURE 6.20 Maximum in transient viscosity after initiation of shear flow versus the duration of a quiescent interval between shearing. The growth of the overshoot peak is caused by reentanglement of the solution. The inset shows representative transient shear stress data (Roland and Robertson, 2006).

much literature devoted to these topics (Chapter 8 herein; Robertson and Roland, 2008; Carbon Black-Polymer Composites, 1982; Hamed, 2000, 2007; Heinrich et al., 2002; Waddell and Evans, 1996; Medalia, 1987). More recently attention has been directed to nanoparticles, such as carbon nanotubes, nanosilicates, etc., as a replacement for conventional fillers (Nah et al., 2010; Bhattacharya et al., 2008). The expectation is that their enormous surface to volume ratio will enable polymer reinforcement to be achieved with very low levels of a nanofiller.

(i) *Payne Effect*

In a carbon black reinforced elastomer, the aggregates (fused primary particles) can agglomerate (floculate) to produce a filler network that gives rise to higher electrical conductivity (Medalia, 1986; Roland et al., 2004; Nikiel et al., 2009) and a modulus that decreases with strain (Chapter 8 herein; Payne, 1962, 1963, 1964; Roland, 1990). Strain breaks up the floculated network structure, as seen in the strain-dependence of the dynamic modulus in Figure 6.22 (Robertson et al., 2007). This network strain-induced breakup is governed by the strain energy; that is, for different concentrations or types of filler, and for different strain modes and frequencies, the maximum in the loss, associated with network disruption, occurs at the same value of the product of dynamic modulus times strain (Robertson and Wang, 2005; Wang and Robertson, 2005). This phenomenon is illustrated in Figure 6.23 for polybutadiene reinforced with different types of fillers (Robertson et al., 2007).

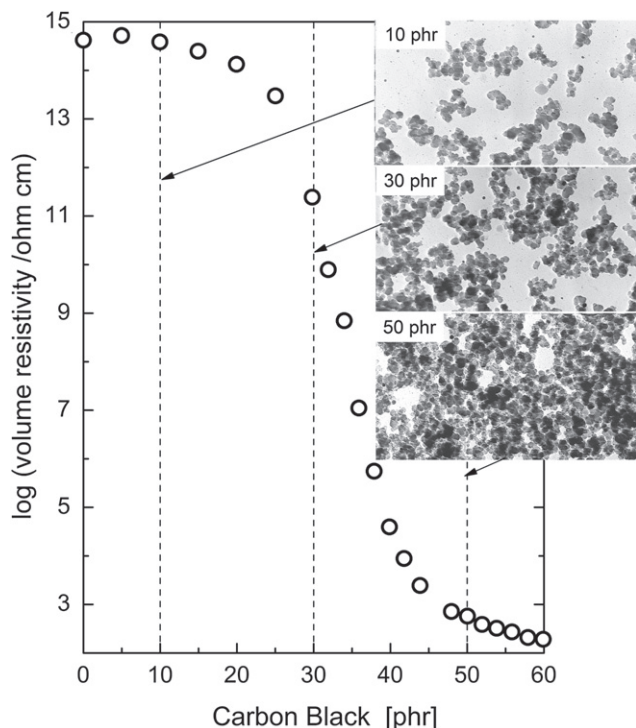


FIGURE 6.21 Change in electrical resistivity of an SBR versus the concentration of N330 carbon black. The property change reflects the degree of particle agglomeration, as seen in the transmission electron micrographs (Nikiel et al., 2009).

At higher strains the network structure is gone, and absent the Payne effect, the main mechanism affecting the processing and flow of filled rubber is the strain amplification in the polymer chains resulting from the inextensibility of the particles. This can be described by the Guth-Gold equation (Guth, 1945; Kohls and Beaucage, 2002):

$$\eta = \eta_0(1 + 2.5\varphi + 14.1\varphi^2), \quad (6.50)$$

where η_0 is the viscosity of the gum rubber and φ is the filler volume fraction. As pointed out by Medalia (1967, 1972), in order for Eq. (6.50) to reproduce experimental results, φ may be augmented by occluded rubber that enhances the hydrodynamic effect of the particles.

(ii) Mullins Effect

It is widely believed that the presence of carbon black or other reinforcing fillers introduces substantial mechanical hysteresis into rubber. Certainly stresses during retraction are lower than during the initial stretching of a rubber, a

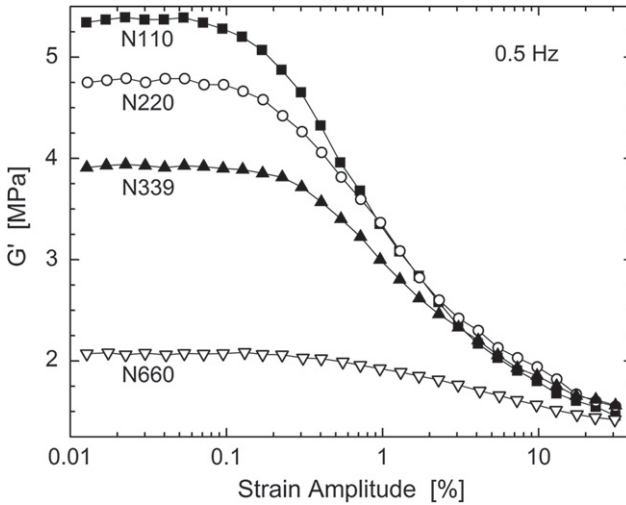


FIGURE 6.22 Storage modulus versus shear strain for 1,4-polybutadiene with 50 phr (18% by volume) of different carbon blacks (Robertson et al., 2007).

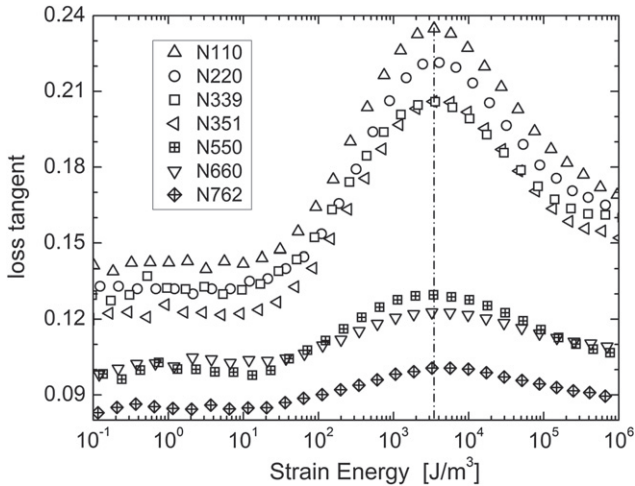


FIGURE 6.23 Loss tangent versus dynamic strain energy for 1,4-polybutadiene with 50 phr of the indicated carbon black. The peak maxima superpose at a strain energy = 3.5 kJ/m^3 , that is independent of filler particle size (Robertson et al., 2007).

phenomenon referred to as the Mullins effect (Mullins, 1969). However, this strain-softening is a viscoelastic effect; it does not require filler, or chain scission, strain-crystallization, or other quasi-irreversible material changes. This was shown in the original work of Harwood and Schallamach (1967), who

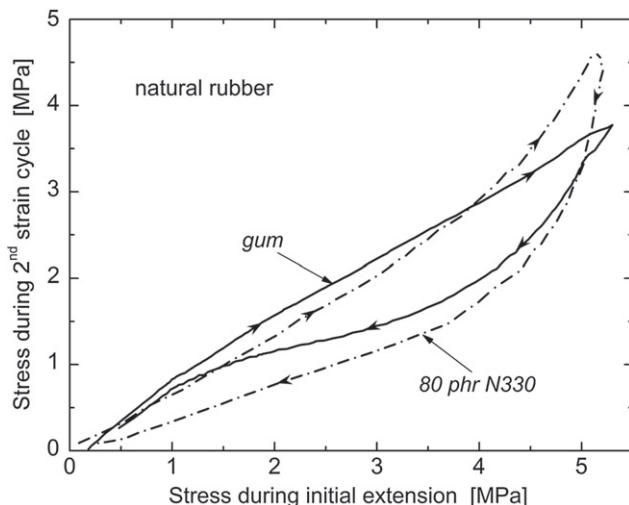


FIGURE 6.24 Hysteresis in unfilled and filled natural rubber networks during the second cycle of tension-retraction. When stretched to the same stress (which requires higher strain in the gum rubber), the softening is roughly equal for the two materials; that is, the softening does not arise primarily due to the reinforcing filler (Harwood and Payne, 1966a,b).

pointed out that when stretched to equivalent stresses, gum and filled elastomers show comparable amounts of softening. Representative data for natural rubber are displayed in Figure 6.24. This strain-softening is not due to the filler network, because disruption of the agglomerated structure transpires at very low strains ($<10\%$ in Figure 6.22). Nevertheless, the mechanical hysteresis of gum rubber during retraction is anomalous, since it is always larger than predictions based on Boltzmann superpositioning (e.g., Eq. (6.30)). Various mechanisms have been suggested as the cause of this Mullins softening, including the contribution from network chain ends or relaxation processes too fast to be included in the constitutive description; however, more work is needed to resolve this issue.

(iii) Nanofillers

At a given concentration, smaller filler particles provide more reinforcement due to the greater interfacial area. This is illustrated in Figure 6.25, showing the increase in bound rubber and tensile strength of a 1,4-polybutadiene as the particle size of the carbon black decreases. Interest has been rekindled recently as part of the burgeoning attention to nanoscience and technology, with carbon nanotubes (Bokobza, 2007; Coleman et al., 2006), silica nanoparticles (Bansal et al., 2005; Bogoslovov et al., 2008), nanoclay (Vu et al., 2001; Sadhu and Bhowmick, 2003; Carretero-Gonzalez et al., 2008), graphene (Stankovich et al., 2006; Wakabayashi et al., 2008), and diamond nanoparticles (Behler et al., 2009) investigated as potential fillers for polymers. Substantial improvements in the

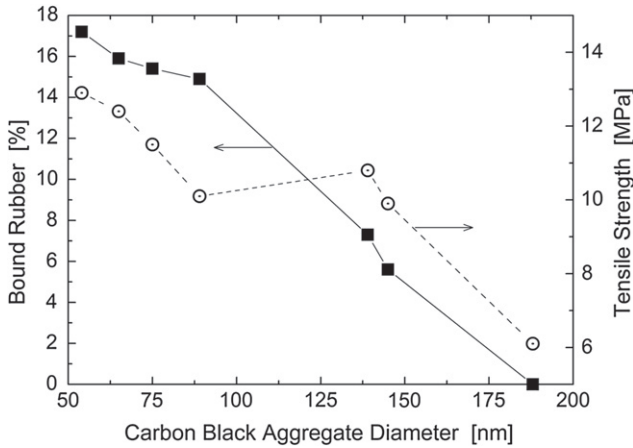


FIGURE 6.25 Bound rubber (squares) and tensile strength (circles) of 1,4-polybutadiene reinforced with 50 phr of carbon black (in order of increasing particle size: N110, N220, N339, N351, N550, N660, and N762) (Robertson et al., 2007).

mechanical properties of polymers can be obtained with a few percent or less of nanofiller (Mark, 2006; Sengupta et al., 2007; Maiti et al., 2008; Vu et al., 2001). An additional factor is the high aspect ratio of particles that are only nm-sized in one or two dimensions. This can augment the reinforcing effect, as seen in Figure 6.26 (Casalini et al., 2012), showing more than two orders

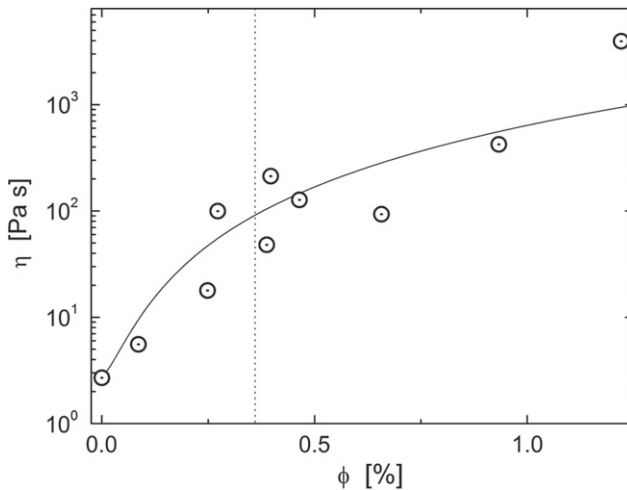


FIGURE 6.26 Dynamic viscosity measured at 0.1 Hz for a polydiamine ($M_W = 4$ kg/mol) as a function of the volume concentration of multiwall carbon nanotubes. The line is the fit to Eq. (6.51) (Casalini et al., 2012).

of magnitude increase in the viscosity with the addition of just 1% carbon nanotubes. To account for this effect of particle shape, the Guth-Gold relation can be modified by introducing a shape factor, f , into Eq. (6.50) (Kohls and Beaucage, 2002):

$$\eta = \eta_0(1 + 2.5f\varphi + 14.1(f\varphi)^2). \quad (6.51)$$

This shape factor affects the interaction among the particles and thus the onset of the Payne effect. The minimum concentration necessary for formation of a particle network can be estimated from (Hobbie and Fry, 2007; Chatterjee and Krishnamoortim, 2007):

$$\varphi^* = \frac{\pi}{4f^2}. \quad (6.52)$$

These equations assume uniform distribution and random orientation of the particles. However, for nanoparticles good mixing can be difficult to achieve, and often chemical modification of the particles is used to enhance their dispersion in the polymer. Poor mixing causes the property changes for small concentrations of nanofillers to be rather modest (Valadares et al., 2006; Bokobza, 2007), much less than the orders of magnitude enhancement seen in Figure 6.26.

6.3.3 Blends

Since flow can disrupt the morphology of a phase-separated blend, the possibility exists for changes in rheological properties. A striking example of this effect is observed in blends with components of different viscosity; the morphology can rearrange during flow to minimize the viscous dissipation (MacLean, 1973). This phase adjustment can cause differences between dynamic viscosities and viscosities measured by flow through capillary dies (Figure 6.27) (Roland and Nguyen, 1988). Only the latter is affected because enrichment of the surface with one component causes slip at the interface, and thus less resistance to flow. Changes in the phase morphology and surface accumulation of one component can be accentuated if there is an attraction (chemisorption) with the processing equipment. This contamination of the walls by one polymer in a blend can result in slippage at the interface, and consequently large reductions in apparent viscosity of the blend (Figure 6.28) (Shih, 1976). Slippage can also result from surface migration of additives in the rubber compound (Ahn and White, 2003, 2004), and it can be induced physically, for example by reducing the hydrostatic pressure (Brzoskowski et al., 1987) or by introducing air between the flowing rubber and the extruder barrel or die (Montes et al., 1988).

Since the effect of filler is nonlinear (Eqs. (6.50) and (6.51)), its proportioning between the phases of an immiscible blend can affect the viscosity and other rheological properties. Carbon black, for example, has greater affinity for the more polar or unsaturated component (Hess, 1991; Lee, 1981), which

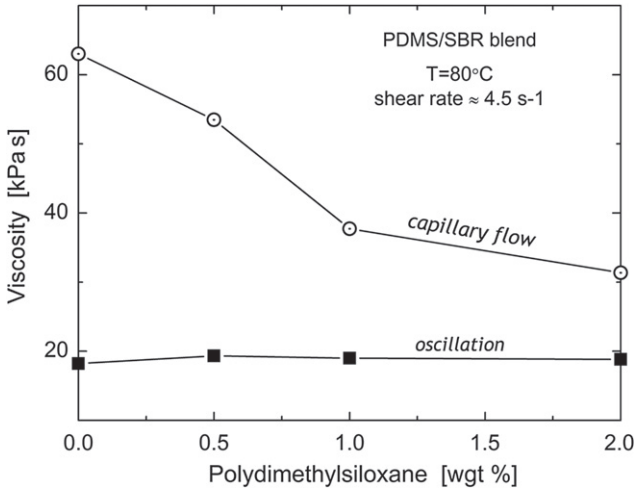


FIGURE 6.27 Viscosity of a blend of styrene-butadiene copolymer and polydimethylsiloxane containing 50 phr N326 carbon black. Presence of the PDMS has no effect on the response to oscillatory strain (squares), but phase segregation and wall slippage occur during flow through a capillary die (circles) (Roland and Nguyen, 1988).

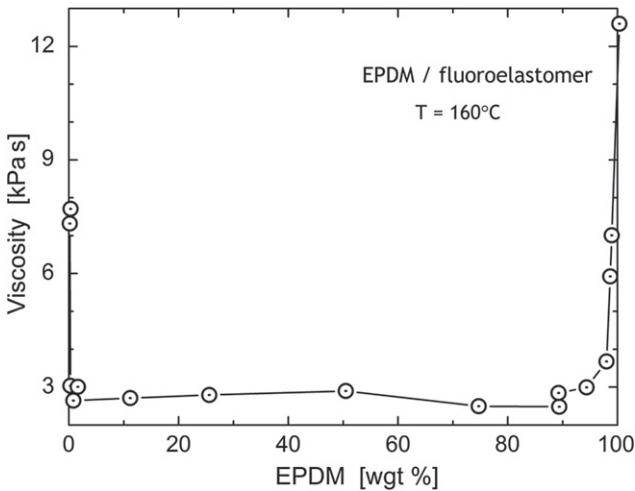


FIGURE 6.28 Apparent viscosity of a blend of EPDM with a fluoroelastomer measured in a capillary rheometer at a shear rate equal to 14 s^{-1} (Shih, 1976).

often leads to a nonuniform distribution. This is seen in Figure 6.29 in the greater uniformity of the respective concentrations of carbon black in the components for SBR blended with a relatively nonpolar component, than when mixed with a polar rubber (Le et al., 2008).

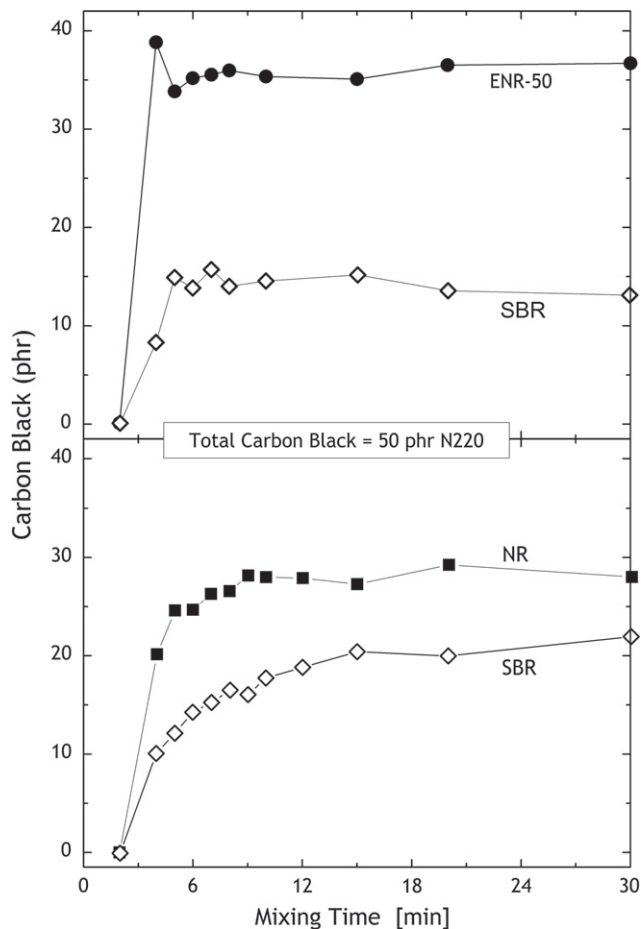


FIGURE 6.29 Respective carbon black contents of the components in immiscible blends of SBR with 50% (top) epoxidized natural rubber and (bottom) natural rubber. The filler preferentially incorporates into the more polar phase (Le et al., 2008).

6.4 ENGINEERING ANALYSIS

6.4.1 Dimensionless Quantities

Dimensional analysis is commonly applied to complex materials and processes to assess the significance of some phenomenon or property regime. It enables analysis of situations that cannot be described by an equation; however, there is no a priori guarantee that a dimensionless analysis will be physically meaningful. Dimensionless quantities are combinations of variables that lack units (i.e., pure numbers), used to categorize the relationship of physical quantities and their interdependence in order to anticipate the behavior. Several dimensionless quantities relevant to polymer rheology and processing are

defined in the following. Although these are all ratios, this is not a requirement of dimensionless quantities; they can be characteristic numbers (e.g., quantum numbers) or represent a count (such as a partition function).

(i) *Reynolds Number*

A very common quantity, this is the ratio of the inertial to viscous forces (Rott, 1990):

$$Re \equiv \frac{\rho v L}{\eta}, \quad (6.53)$$

where ρ is the mass density, v is the velocity, and L is a characteristic dimension. For extensional and shear flows, L represents the dimension parallel and perpendicular, respectively, to the flow. Re can identify the laminar to turbulent flow transition for different fluids and different flow rates, independently of the geometry. For example, for flow in a circular pipe, L is the inside diameter, and the transition from laminar to turbulent flow occurs in the range $2300 < Re < 4000$. A variation on Re is the **Blake Number** (Blake, 1922), which applies to porous media, such as beds of solids.

(ii) *Deborah Number*

The Deborah number is the ratio of the relaxation time of the material to the experimental timescale:

$$De \equiv \dot{\gamma} \tau. \quad (6.54)$$

A larger Deborah number implies a more elastic response. The term, which comes from the biblical quote in Section 6.1.1, was coined by Reiner (1964).

(iii) *Weissenberg Number*

Defined as the ratio of the material relaxation time to the processing time during flow, Wi characterizes the amount of molecular orientation induced by the flow. For simple shear flow, Wi is given by the product of τ times the shear rate. Related to the Deborah number, Wi is used for constant straining, whereas De describes deformations with a varying strain history.

(iv) *Capillary Number*

This quantity is the ratio of the viscous force to the surface tension across an interface,

$$Ca \equiv \frac{\eta v}{\Upsilon}, \quad (6.55)$$

where Υ is the surface tension. Relevant to extensional flow from orifices and domain formation during mixing of immiscible liquids, values of Ca larger than unity imply stretching of dispersed particles or droplets, which is a necessary

condition for their dispersion. The ratio of the Deborah and capillary numbers,

$$\frac{De}{Ca} = \frac{\tau \Upsilon}{\eta L}, \quad (6.56)$$

the “elastocapillary number” (Hsu and Leal, 2009), is a measure of the deformation of dispersed phases that is independent of the strain rate. L in Eq. (6.56) is related to the droplet size.

(v) *Weber Number*

Analogous to the capillary number, We is the ratio of the inertial force to the surface tension across an interface,

$$We \equiv \frac{\rho v^2 L}{\Upsilon}. \quad (6.57)$$

(vi) *Brinkman Number*

This number, used in polymer processing, describes the heat flow between the flowing material and the vessel containing it (e.g., the rotor and walls of an extruder). It is defined as

$$Br \equiv \frac{\eta v^2}{\kappa \Delta T}, \quad (6.58)$$

in which κ is the thermal conductivity of the material and ΔT its temperature difference with the vessel. A large value of $Br (> 1)$ indicates significant viscous heating.

(vii) *Bingham Number*

Used to characterize a polymer that flows when the stress reaches a characteristic level (Bingham, 1916), this number is the ratio of the yield stress, σ_Y , to the viscous stress,

$$Bn \equiv \frac{\sigma_Y L}{\eta v}. \quad (6.59)$$

(viii) *Elasticity Number*

The ratio of the elastic forces to the inertial forces,

$$El = \frac{\tau \eta}{\rho L^2}. \quad (6.60)$$

and equal to the Weissenberg number divided by the Reynolds numbers, El characterizes the effect of elasticity on the flow. For a polymer solution El depends only on the material properties, except for the size of the flow device.

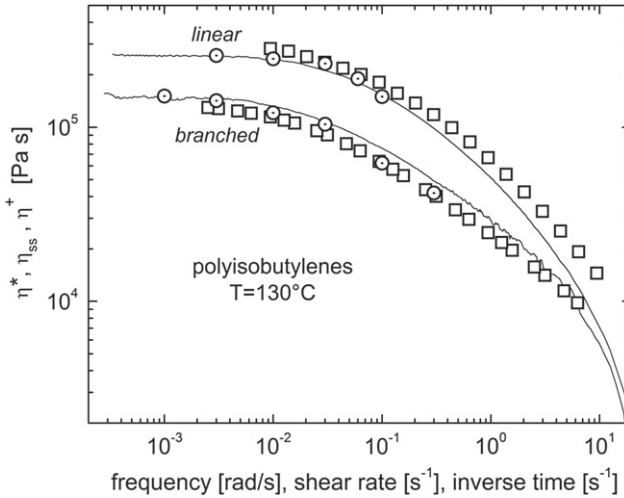


FIGURE 6.30 Dynamic viscosity (squares), steady-state shear viscosity (circles), and the transient viscosity calculated using Eq. (6.65) (solid lines) for a linear ($M_W = 389$ kg/mol) and a highly branched ($M_W = 1080$ kg/mol) with 21 branches per chain and a branch $M_W = 52.7$ kg polyisobutylene (Robertson et al., 2002).

6.4.2 Empirical Rules

(i) Cox-Merz Rule (Cox and Merz, 1958)

The Cox-Merz rule states that the shear-rate dependence of the steady-state viscosity equals the frequency dependence of the complex viscosity,

$$\eta(\dot{\gamma}) = \eta(\dot{\gamma})|_{\omega=\dot{\gamma}}, \quad (6.61)$$

in which $\dot{\gamma}$ is the strain rate. The upper panel of Figure 6.19 (Robertson et al., 2004) shows data for an entangled solution of 1,4-polybutadiene, and in Figure 6.30 (Robertson et al., 2002) are data for linear and branched polyisobutylene; both materials exhibit good compliance with Eq. (6.61). However, the presence of filler degrades the connection between the two viscosities, as shown in Figure 6.31 for a polydimethylsiloxane (Xu et al., 2008). The data for gum silicone rubber agree well with the Cox-Merz rule, but filler causes the steady shear viscosities to be smaller, presumably reflecting breakup of the agglomerated filler structure under continuous shearing conditions.

(ii) Laun Relations (Laun, 1986)

Laun proposed two equations relating the dynamic storage and loss moduli to the first normal stress difference coefficient for steady shearing:

$$\Psi_1(\dot{\gamma}) = 2G' \omega^{-2} \left[1 + (G'/G'')^2 \right]^a \Big|_{\omega=\dot{\gamma}} \quad (6.62)$$

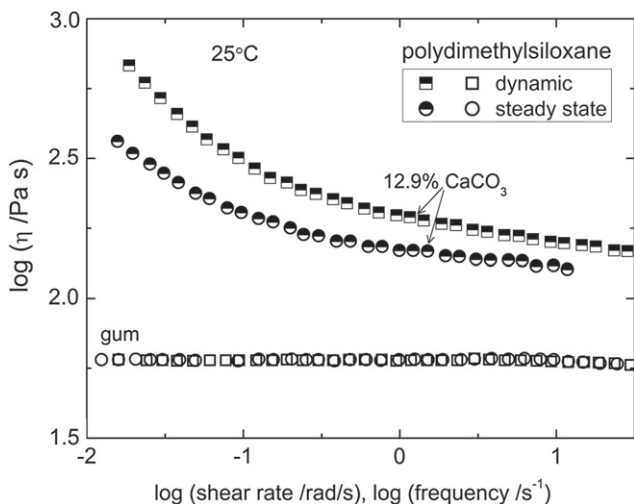


FIGURE 6.31 Dynamic viscosity (squares) and steady-state viscosity (circles) for PDMS with the indicated concentration by volume of calcium carbonate (half-filled symbols) and without filler (open symbols) (Xu et al., 2008).

and to the steady-state recoverable strain,

$$\gamma_{\text{rec}}(\dot{\gamma}) = (G'/G'') \left[1 + (G'/G'')^2 \right]^{1.5} \Big|_{\omega=\dot{\gamma}}. \quad (6.63)$$

In Eq. (6.62) the exponent a is taken as a fitting parameter having a value around 0.7. The accuracy of these expressions is not quantitative (Roland, 2011). From the definitions of the dynamic moduli in the terminal region (Eqs. (6.23) and (6.24), the first Laun relation reduces to the equation of Coleman and Markovitz (1964),

$$\psi_1^0 = \lim_{\dot{\gamma} \rightarrow \infty} \frac{N_1(\dot{\gamma})}{\dot{\gamma}} = 2J_s^0 \eta_0^2, \quad (6.64)$$

which is valid only for low shear rates.

(iii) Gleissle Equations (Gleissle, 1980)

This empirical equation connects the steady-state viscosity to the transient viscosity, $\eta^+(t)$, measured from the stress growth during approach to steady state at the limiting (Newtonian) shear rate,

$$\lim_{\dot{\gamma} \rightarrow 0} \eta^+(t, \dot{\gamma}) = \eta(\dot{\gamma}) \quad (t^{-1} = \dot{\gamma}). \quad (6.65)$$

As illustrated in Figure 6.19 (upper panel) (Robertson et al., 2004) and Figure 6.30 (Robertson et al., 2002), Eq. (6.65) is only approximate; nevertheless, using it enables estimates for the viscosity over a broad range of rates from a single measurement of stress versus time at one slow shear rate.

(iv) *Lodge-Meissner Rule (Lodge and Meissner, 1972)*

After imposition of a step strain, the ratio of the first normal stress difference, N_1 , to the shear stress is equal to the strain, or

$$N_1(t) = \varepsilon^2 G(t) = \varepsilon \sigma(t). \quad (6.66)$$

This behavior is apparent in the top panel of Figure 6.17, showing that the birefringence perpendicular to the strain direction has the same time-dependence as the stress.

(v) *Boyer-Spencer (Boyer and Spencer, 1944) and Simha-Boyer (Simha and Boyer, 1962) Rules*

From analysis of data for various polymers, two correlations have been reported concerning properties at the glass transition. The rationalization for both relies on a free volume description of the glass transition in polymers, which means the correlations are strictly empirical. The Boyer-Spencer rule (Boyer and Spencer, 1944) posits that the product of the glass transition temperature and the thermal expansion coefficient at T_g is a universal constant, $\alpha_P T_g = 0.113$. An alternative analysis of Bondi (Van Krevelen, 1990) gives $\alpha_P T_g = 0.116$. The data in Figure 6.32 (Krause et al., 1965) show that this empirical rule is reasonably accurate, with a mean for 51 amorphous polymers yielding $\alpha_P T_g = 0.162 \pm 0.005$. This correlation is affirmed by the density scaling property (Eq. (6.40)), from which a relation between γ and the ratio of the isochoric and isobaric activation energies can be derived (Casalini and Roland, 2004a):

$$\frac{E_V}{E_P} = (1 + \alpha_P T \gamma)^{-1}, \quad (6.67)$$

where the isobaric activation energy (which is more properly called an activation enthalpy) has its usual definition,

$$E_P(T, P) = R \left. \frac{\partial \ln \tau}{\partial T^{-1}} \right|_P, \quad (6.68)$$

and the activation energy at constant density is

$$E_V(T, V) = R \left. \frac{\partial \ln \tau}{\partial T^{-1}} \right|_V. \quad (6.69)$$

E_V/E_P can be calculated from segmental relaxation times for polymers and rotational correlation times of molecular liquids, measured over a range of thermodynamic conditions. Plots of the activation energy ratio versus γ can be fit using a value of $\alpha_P T_g = 0.18 \pm 0.01$ (Casalini and Roland, 2004b), consistent with the Boyer-Spencer rule.

According to the Simha-Boyer rule (Simha and Boyer, 1962), the product of the T_g times the change in thermal expansivity at T_g is a material-independent

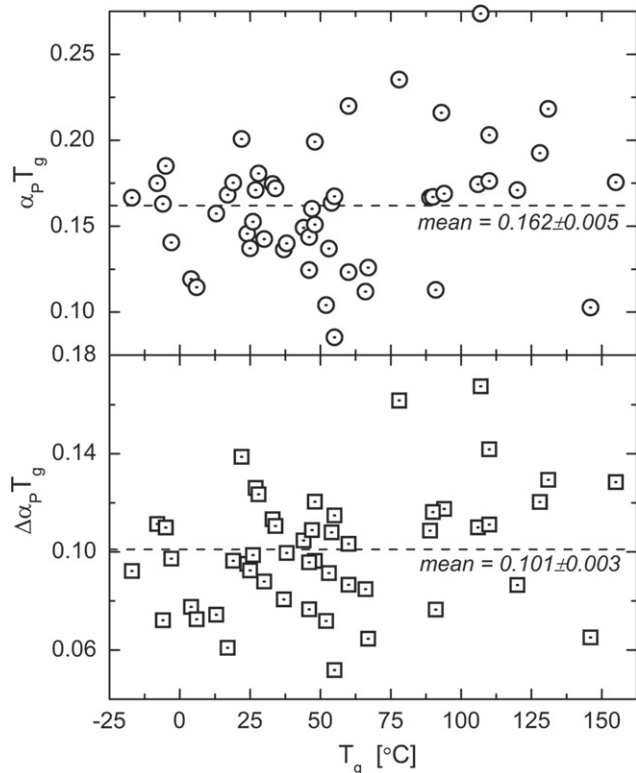


FIGURE 6.32 (Top) Product of the glass transition temperature and the thermal expansion coefficient of the rubber at T_g for 51 polymers. (Bottom) Product of T_g and the difference in thermal expansivity of the rubber and glassy states for the same materials. The data fall close to the respective predictions of the Boyer-Spencer and Simha-Boyer rules (Section (v)) (Krause et al., 1965).

constant, $\Delta\alpha T_g = 0.113$. This prediction has been tested by different groups and found to be fairly accurate (Krause et al., 1965; Abeliiov et al., 1979). Results are displayed in Figure 6.32 for 51 polymers, yielding $\Delta\alpha T_g = 0.101 \pm 0.003$.

6.5 PRACTICAL PROCESSING CONSIDERATIONS

6.5.1 Mixing

There are two main aspects to mixing—distributive mixing, to combine the ingredients and obtain a spatially uniform composition, and dispersive mixing, which refers to the breakup of constituents into smaller sizes. The latter presents the greater challenge. The general principle is that the obtained dispersed particle size depends both on the rheological properties of the materials and the type of mixing. Concerning the rheological properties, lower cohesive

strength of the dispersed component and a closer matching of its viscosity (assuming fluid particles) to that of the matrix leads to more effective dispersion (Rallison, 1984; Grace, 1982; Nelson et al., 1977). The type of mixing affects the dispersion process primarily because stretching flows are most effective at dispersion and rotational flows are completely ineffective. In order to sustain the stresses and thereby fracture the particle, flow field vorticity should be suppressed, since reorientation of the particles or domains allows the stresses to successively counterbalance each other. Beyond this consideration, the objective is to apply the highest stresses and strain rates, provided degradation (chain scission) is not an issue, and to ensure that all the material passes through the regions of the mixing vessel at which dispersion forces are greatest. Very generally, the strain rate tensor can be written as

$$\Gamma \equiv \nabla_v = \begin{pmatrix} \frac{\partial v_x}{\partial x} & \frac{\partial v_x}{\partial y} & \frac{\partial v_x}{\partial z} \\ \frac{\partial v_y}{\partial x} & \frac{\partial v_y}{\partial y} & \frac{\partial v_y}{\partial z} \\ \frac{\partial v_z}{\partial x} & \frac{\partial v_z}{\partial y} & \frac{\partial v_z}{\partial z} \end{pmatrix}. \quad (6.70)$$

A metric for the strength of the flow field, ζ , can be introduced, where $\zeta = 1$ for pure extensional flow and -1 for rotation (Fuller and Leal, 1981). The strength of the flow field is then given by the ratio of the stretching to the vorticity, equal to $\frac{1 + \zeta}{1 - \zeta}$. For two-dimensional flow (Fuller and Leal, 1981),

$$\Gamma = \frac{\dot{\gamma}}{2} \begin{pmatrix} (1 + \zeta) & (1 - \zeta) & 0 \\ (-1 + \zeta) & (-1 - \zeta) & 0 \\ 0 & 0 & 0 \end{pmatrix}, \quad (6.71)$$

where $\dot{\gamma}$ represents the local velocity gradient. An arbitrary flow field can be expressed as the linear superposition of pure stretching and rotational flow, with shear flow corresponding to $\zeta = 0$. Using their strength criteria, more dispersion will occur on the entrance to a capillary die, associated with ζ close to unity, than for shearing flow through the die. The effect of slippage of the polymer is to reduce the velocity gradient; thus (Fuller and Leal, 1981),

$$\Gamma_{\text{eff}} = \frac{\dot{\gamma}}{2} \begin{pmatrix} (1 - \xi)(1 + \zeta) & (1 - \zeta) & 0 \\ (-1 + \zeta) & -(1 - \xi)(-1 - \zeta) & 0 \\ 0 & 0 & 0 \end{pmatrix}, \quad (6.72)$$

with ξ a measure of the slippage. The strength of the flow field is now given by $\frac{(1 - \xi)(1 + \zeta)}{1 - \zeta}$.

These considerations apply both to mixing of the components of a polymer blend and to dispersion of particulate fillers. For blends the obtained size of the

dispersed phase represents the competition between breakup of the particles and their flow-induced coalescence (Roland and Bohm, 1984; Sirisinha et al., 2003; Chen et al., 2006; Peng et al., 2011). Similarly, the final degree of filler dispersion depends not only on the breakup of the aggregates during mixing, but also on the extent of reagglomeration, which occurs, for example, during curing or thermal annealing (Bohm and Nguyen, 1995; Mihara et al., 2009; Schwartz et al., 2003). Chemical treatment of the filler surface is a common method to suppress agglomeration, either with coupling agents that promote interaction with the polymer, or using shielding agents to decrease filler-filler interactions (Robertson et al., 2008; Ye et al., 2012; Lin et al., 2010).

6.5.2 Die Swell

When rubber is deformed during processing operations such as extrusion or calendaring, its inherent elasticity will cause some subsequent recovery. A fundamental material constant characterizing this tendency is J_s^0 , defined in Eqs. (6.12) and (6.14). Elastic recovery is also reflected in die swell, \hat{D} , defined as the ratio of the final and initial dimensions perpendicular to the flow. Die swell is governed by the normal force, although predictions of \hat{D} for an arbitrary deformation are not possible. However, for steady-state flow there are approximate relations between \hat{D} and the first (primary) normal force (Tanner, 1970),

$$N_1 = 2\sigma(2\hat{D}^6 - 2)^{1/2}, \quad (6.73)$$

and (Bagley and Duffey, 1970),

$$N_1 = 2\sigma(2\hat{D}^4 - \hat{D}^{-2}). \quad (6.74)$$

Substituting for the stress in Eq. (6.66), \hat{D} can be related to the shear strain, or using Eq. (6.62) to the dynamic modulus. Results are shown in Figure 6.33 (Müllner et al., 2008), comparing the die swell measured in a capillary rheometer to values calculated from dynamic measurements. The rough agreement with experimentally measured die swell is satisfactory given the approximate nature of the derivation of Eqs. (6.73) or (6.74) (Tanner, 1970; Bagley and Duffey, 1970).

As mentioned in Section 6.3.3, the affinity of filler for a rubber is expected to be greater for more polar rubbers and those having a higher degree of unsaturation, and this can result in a nonuniform distribution of the filler between the phases of a blend (Hess, 1991; Lee, 1981; Le et al., 2008). Since active fillers such as carbon black interact with the polymer chains, mainly via chemisorption, there is little migration between the phases. This means that a nonuniform distribution can be obtained by design, through the sequence in which the materials are added to the mixing. Properties such as the elasticity depend nonlinearly on the filler content, which means a rubber blend having a nonuniform distribution can behave differently than one in which the filler

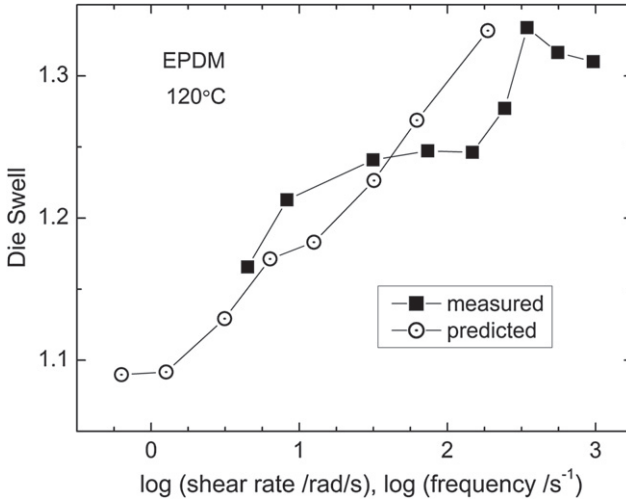


FIGURE 6.33 \hat{D} measured for a filled EPDM rubber (squares) and calculated from dynamic mechanical measurements (circles) (Müllner et al., 2008).

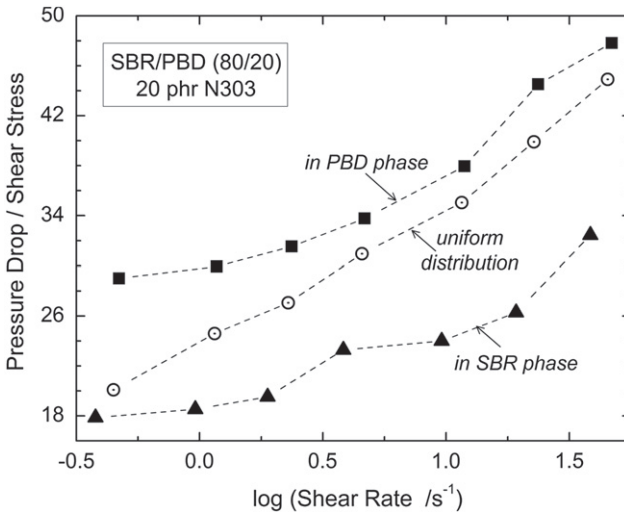


FIGURE 6.34 Exit pressure normalized by the shear stress for an 80:20 blend of styrene-butadiene copolymer with 1,4-polybutadiene, containing 20 phr of carbon black. The polymers and filler were added to the mixer simultaneously (circles), or the filler was first mixed into either the SBR (triangles) or the PBD (squares). The greatest extrudate swell is observed when the major phase lacks filler (Lee, 1981).

is equally partitioned between components. Figure 6.34 (Lee, 1981) shows the pressure drop when a rubber blend exits a die; this exit pressure is a measure of the elasticity and hence of extrudate swell. By incorporating the carbon black into the major component, the exit pressure is smaller than for a uniform

distribution of the filler. On the other hand, if the carbon black is mixed into the minor component, the large elasticity of the “gum” phase results in very large exit pressures.

6.5.3 Tack

The ability of uncured rubber to adhere quickly to itself and then be resistant to separation is known as tack or autohesion. Tack can be crucial to the assembly of rubber components that need to remain in place prior to vulcanization. An example is tire assembly, which entails positioning carcasses, belts, and other plies; these layers are held together by virtue of their tack. There are three requirements for “building tack”:

- The surfaces must attain microscopic contact to allow interpenetration of chains via diffusion. This surface wetting depends on the surface roughness and the rubber viscosity.
- The ensuing interdiffusion must transpire rapidly, to fuse the layers and yield adequate adhesion.
- The cohesive strength of the rubber must be sufficient, since it serves as an upper bound on the achievable autohesion (Hamed and Shieh, 1986).

Plasticization of the compound facilitates the first two processes; however, it entails loss of green strength and thus it is not usually an effective means to improve tack. Tackifying resins, which are important ingredients in pressure-sensitive adhesives such as Scotch tape, can be employed in rubber formulations to take advantage of the stronger rate dependence the resins impart to the mechanical response (Hamed and Roberts, 1994; Basak et al., 2012). At high strain rates, corresponding to peeling the layers apart, these resins solidify the material, whereas their effect on the viscosity at the slow strain rates relevant to wetting is less significant. Strain-crystallizing rubbers, such as natural rubber, exhibit superior tack due to the dependence of their viscosity and strength on strain. Only at the large strains ($\sim 200\%$ (Choi and Roland, 1997)) that induce crystallization does the material have strong resistance to flow. At low strains relevant to coalescence of the two surfaces, the rubber is amorphous and thus has the compliance necessary for intimate contact to develop between adherends.

The adhesive strength and failure mode can change with both the contact time and the rate at which the surfaces are separated (Hamed and Wu, 1995; Schach and Creton, 2008). Under the usual conditions, the process of interdiffusion causes an increase in the tack with contact time. When the diffusion has transpired over distances on the order of the chain coil size, the interfacial region becomes indistinguishable from the bulk material, and the tack becomes constant, equal to the cohesive strength of the rubber. The coil size of a typical rubber molecule is in the range from 10 to 20 nm. For typical self-diffusion constants of rubbery polymers at room temperature, ca. $0.4\text{--}4\text{ nm}^2/\text{s}$

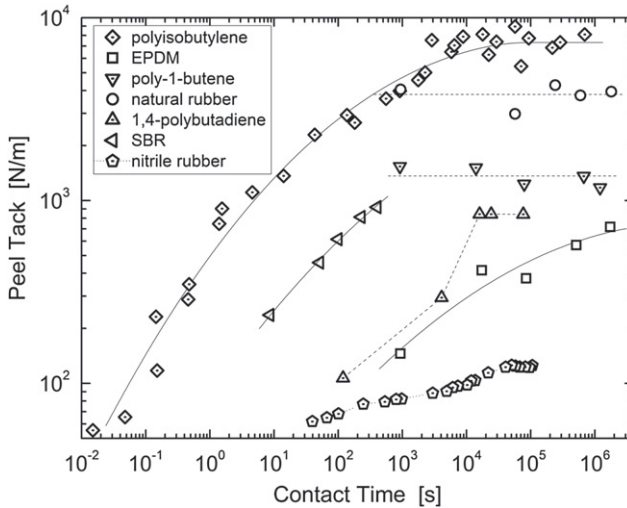


FIGURE 6.35 Peel force per unit length (equal to the detachment energy per unit area) measured for various rubbers versus contact time. The increase is due to the buildup of an interfacial layer, as the chains interdiffuse. Some polymers (natural rubber and poly-1-butene (hydrogenated 1,2-polybutadiene)) show no time-dependence because interdiffusion is fast relative to the measurement time. For polyisobutylene, 1,4-polybutadiene, and an acrylonitrile-butadiene copolymer, the cohesive strength of the materials is attained at longer contact times. For the styrene-butadiene copolymer and ethylene-propylene-diene terpolymer, complete interdiffusion is never complete, and the adhesion continues to increase with time. Of course, the ultimate level of tack and the adhesion kinetics are strongly dependent on molecular weight. The ordinate values for SBR and NBR were shifted for clarity (Skewis, 1966; Roland and Bohm, 1985; Bothe and Rehage, 1982).

(Skewis, 1966; Roland and Bohm, 1985; Bothe and Rehage, 1982), a plateau value of tack is thus expected in time periods ranging from seconds to several minutes. Results for a number of rubbers are in accord with this expectation (Figure 6.35).

ACKNOWLEDGMENT

This work was supported by the Office of Naval Research.

REFERENCES

- Abdel-Goad, M., Pyckhout-Hintzen, W., Kahle, S., Allgaier, J., Richter, D., Fetters, L.J., 2004. *Macromolecules* 37, 8135.
- Abeliov, Y.A., Nikolskii, V.G., Kirillov, V.N., Alekseyev, B.F., 1979. *Polym. Sci. USSR* 20, 2590.
- Ahn, S., White, J.L., 2003. *J. Appl. Polym. Sci.* 90, 1555; Ahn, S., White, J.L., 2004. *J. Appl. Polym. Sci.* 91, 651.
- Andrews, R.D., Tobolsky, A., 1951. *J. Polym. Sci.* 1, 221.
- Angell, C.A., 1991. *Pure Appl. Chem.* 63, 1387.

- Angell, C.A., Ngai, K.L., McKenna, G.B., McMillan, P.F., 2000. *J. Appl. Phys.* 88, 3113.
- Arruda, E., Wang, Y., Przbylo, P., 2001. *Rubber Chem. Technol.* 74, 560.
- Ashurst, W.T., Hoover, W.G., 1975. *Phys. Rev. A* 11, 658.
- Attane, P., Pierrard, J.M., Turrel, G., 1985. *J. Non-Newton. Fluid Mech.* 18, 295.
- Bagley, E.B., Duffey, H.J., 1970. *Trans. Soc. Rheol.* 14, 545.
- Bair, S., 2002. *J. Eng. Tribol.* 216, 1.
- Bair, S., Winer, W.O., 1980. *J. Lubricat. Technol.* 102, 229.
- Baird, D.G., Collias, D.I., 1998. *Polymer Processing: Principles and Design.* Wiley-Interscience.
- Balasubramanian, V., Bush, K., Smoukov, S., Venerus, D.C., Schieber, J.D., 2005. *Macromolecules* 38, 6210.
- Bansal, A., Yang, H.C., Li, C.Z., Cho, K.W., Benicewicz, B.C., Kumar, S.K., Schadler, L.S., 2005. *Nat. Mater.* 4, 693.
- Bardik, V.Y., Sysoev, V.M., 1998. *Low Temp. Phys.* 24, 601.
- Basak, G.C., Bandyopadhyay, A., Bhowmick, A.K., 2012. *J. Mater. Sci.* 47, 3166.
- Batzler, H., Wagner, M.H., Meissner, J., 1980. *Makromol. Chem.* 181, 1533.
- Behler, K.D., Stravato, A., Mochalin, V., Korneva, G., Yushin, G., Gogotsi, Y., 2009. *ACS Nano.* 3, 363.
- Bergstrom, J.S., Boyce, M.C., 1998. *J. Mech. Phys. Solids* 46, 931.
- Bernstein, B., Kearsley, E.A., Zapas, L.J., 1963. *Trans. Soc. Rheol.* 7, 391.
- Bernstein, B., Kearsley, E.A., Zapas, L.J., 1964. *J. Res. Natl. Bur. Stand., Sect. B* 68, 103.
- Berry, G.C., 2003. *Polymer Rheology: Principles, Techniques and Applications.* In: Brady, J.R.F. (Ed.), *Desk Reference of Polymer Characterization and Analysis.* American Chemical Society, New York, p. 574.
- Berry, G.C., Fox, T.G., 1968. *Adv. Polym. Sci.* 5, 261.
- Bhattacharya, M., Maiti, M., Bhowmick, A.K., 2008. *Rubber Chem. Technol.* 81, 782.
- Bingham, E.C., 1916. *US Bureau Stand. Bull.* 13, 309.
- Blake, F.C., 1922. *Trans. AIChE* 14, 415.
- Boese, D., Momper, B., Meier, G., Kremer, F., Hagenah, I.U., Fischer, E.W., 1989. *Macromolecules* 22, 4416.
- Bogoslovov, R.B., Roland, C.M., Ellis, A.R., Randall, A.M., Robertson, C.G., 2008. *Macromolecules* 41, 1289.
- Bogoslovov, R.B., Hogan, T.E., Roland, C.M., 2010. *Macromolecules* 43, 2904.
- Bohm, G.G.A., Nguyen, M.N., 1995. *J. Appl. Polym. Sci.* 55, 1041.
- Bohmer, R., Ngai, K.L., Angell, C.A., Plazek, D.J., 1993. *J. Chem. Phys.* 99, 4201.
- Bokobza, L., 2007. *Polymer* 48, 4907.
- Boltzmann, L., 1874. *Sitzungsber. Kaiserl. Akad. Wiss. Wien* 70, 275.
- Bothe, L., Rehage, G., 1982. *Rubber Chem. Technol.* 55, 1308.
- Boyer, R.F., Spencer, R.S., 1944. *J. Appl. Phys.* 15, 398.
- Brochard, F., De Gennes, P.G., 1977. *Macromolecules* 10, 1157.
- Brzoskowski, R., White, J.L., Szydowski, W., Weissert, F.C., Nakajima, N., Min, K., 1987. *Rubber Chem. Technol.* 60, 945.
- Carretero-Gonzalez, J., Retsos, H., Verdejo, R., Toki, S., Hsiao, B.S., Giannelis, E.P., Lopez-Manchado, M.A., 2008. *Macromolecules* 41, 6763.
- Casalini, R., Roland, C.M., 2004a. *Phys. Rev. E* 69, 062501.
- Casalini, R., Roland, C.M., 2004b. *Coll. Polym. Sci.* 283, 107.
- Casalini, R., Roland, C.M., 2005. *Macromolecules* 38, 1779.
- Casalini, R., Bogoslovov, R., Qadri, S.B., Roland, C.M., 2012. *Polymer* 53, 1282.
- Chandler, D., Weeks, J.D., Andersen, H.C., 1983. *Science* 220, 787.
- Chang, I., Sillescu, H., 1997. *J. Phys. Chem. B* 101, 8794.
- Chang, W.V., Bloch, R., Tschoegl, N.W., 1976. *Rheol. Acta* 15, 367.
- Chapter 3 herein.
- Chapter 8 herein.
- Chatterjee, T., Krishnamoortim, R., 2007. *Phys. Rev. E* 75, 050403.
- Chen, X., Xi, J., Guo, B.H., 2006. *J. Appl. Polym. Sci.* 102, 3201.
- Choi, I.S., Roland, C.M., 1997. *Rubber Chem. Technol.* 70, 202.
- Cohen, M.H., Grest, G.S., 1979. *Phys. Rev. B* 20, 1077.
- Cohen, M.H., Grest, G.S., 1984. *J. Non-Cryst. Solids* 61–62, 749.
- Cohen, M.H., Turnbull, D., 1959. *J. Chem. Phys.* 31, 1164.

- Colby, R.H., Fetters, L.J., Graessley, W.W., 1987. *Macromolecules* 20, 2237.
- Colby, R.H., Rubinstein, M., Viovy, J.L., 1992. *Macromolecules* 25, 996.
- Coleman, B.D., Markovitz, H., 1964. *J Appl. Phys.* 35, 1.
- Coleman, B.D., Zapas, L.J., 1989. *J. Rheol.* 33, 501.
- Coleman, J.N., Khan, U., Blau, W.J., Gunko, Y.K., 2006. *Carbon* 44, 1624.
- Colmenero, J., Alegria, A., Alberdi, J.M., Alvarez, F., Frick, B., 1991. *Phys. Rev.* B44, 7321.
- Colmenero, J., Alegria, A., Santangelo, P.G., Ngai, K.L., Roland, C.M., 1994. *Macromolecules* 27, 407.
- Corezzi, S., Rolla, P.A., Paluch, M., Ziolo, J., Fioretto, D., 1999. *Phys. Rev. E* 60, 4444.
- Cox, W.P., Merz, E.H., 1958. *J. Polym. Sci.* 28, 619.
- Danusso, F., Levi, M., Gianotti, G., Turri, S., 1993. *Polymer* 34, 3687.
- Dealy, J.M., Tsang, W.K.-W., 1981. *J. Appl. Polym. Sci.* 26, 1149.
- de Gennes, P.-G., 1979. *Scaling Concepts in Polymer Physics*. Cornell University, Ithaca.
- DeKee, D., Fong, C.F.C.M., 1994. *Polym. Eng. Sci.* 34, 438.
- Ding, Y.F., Sokolov, A.P., 2006. *Macromolecules* 39, 3322.
- Doi, M., 1980. *J. Polym. Sci. Polym. Phys. Ed.* 18, 1891; 18, 2055 (1980).
- Doi, M., Edwards, S.F., 1986. *The Theory of Polymer Dynamics*. Clarendon Press, Oxford.
- Doolittle, A.K., Doolittle, D.B., 1957. *J. Appl. Phys.* 28, 901.
- Everaers, R., Sukumaran, S.K., Grest, G.S., Svaneborg, C., Sivasubramanian, A., Kremer, K., 2004. *Science* 303, 823.
- Ferry, J.D., 1980. *Viscoelastic Properties of Polymers*, third ed. Wiley, New York.
- Ferry, J.D., Grandine, L.D., Fitzgerald, E.R., 1953. *J. Appl. Phys.* 24, 911.
- Fetters, L.J., Lohse, D.J., Richter, D., Witten, T.A., Zirkel, A., 1994. *Macromolecules* 27, 4639.
- Fetters, L.J., Lohse, D.J., Milner, S.T., Graessley, W.W., 1999. *Macromolecules* 32, 6847.
- Fetters, L.J., Lohse, D.J., Graessley, W.W., 1999. *J. Polym. Sci. Polym. Phys. Ed.* 3, 1023.
- Fetters, L.J., Lohse, D.J., Garcia-Francok, C.A., Brant, P., Richter, D., 2002. *Macromolecules* 35, 10096.
- Fillers, R.W., Tschoegl, N.W., 1977. *Trans. Soc. Rheol.* 21, 51.
- Fischer, E.W., Donth, E., Steffen, W., 1992. *Phys. Rev. Lett.* 68, 2344.
- Fitzgerald, E.R., Grandine, L.D., Ferry, J.D., 1953. *J. Appl. Phys.* 24, 650.
- Floudas, G., 2003. Chapter 8 in *Kremer and Schonhals*.
- Fragiadakis, D., Roland, C.M., 2011. *Phys. Rev. E* 83, 031504.
- Fragiadakis, D., Casalini, R., Bogoslovov, R.B., Robertson, C.G., Roland, C.M., 2011. *Macromolecules* 44, 1149.
- Fuller, K.N.G., 1988. In: Roberts, A.D. (Ed.), *Natural Rubber Science and Technology*. Oxford, New York.
- Fuller, G.G., Leal, L.G., 1981. *J. Polym. Sci. Polym. Phys. Ed.* 19, 557.
- Gerhardt, L.J., Manke, C.W., Gulari, E., 1997. *J. Polym. Sci. Polym. Phys.* 35, 523.
- Gleissle, W., 1980. In: Astarita, G., Marucci, G., Nicolais, L. (Eds.), *Rheology*, vol. 2. Plenum, New York, p. 457.
- Goldstein, M.J., 1969. *J. Chem. Phys.* 51, 3728.
- Grace, H.P., 1982. *Chem. Eng. Comm.* 14, 225.
- Graessley, W.W., 2008. *Polymeric Liquids and Networks: Dynamics and Rheology*. Taylor & Francis, London.
- Graessley, W.W., Edwards, S.F., 1981. *Polymer* 22, 1329.
- Grest, G.S., Cohen, M.H., 1981. *Adv. Chem. Phys.* 48, 455.
- Guth, E., 1945. *J. Appl. Phys.* 16, 20.
- Hamed, G.R., 2000. *Rubber Chem. Technol.* 73, 524.
- Hamed, G.R., 2007. *Rubber Chem. Technol.* 80, 533.
- Hamed, G.R., Roberts, G.D., 1994. *J. Adhes.* 47, 95.
- Hamed, G.R., Shieh, C.H., 1986. *Rubber Chem. Technol.* 59, 883.
- Hamed, G.R., Wu, P.S., 1995. *Rubber Chem. Technol.* 68, 248.
- Han, C.D., Ma, C., 1983. *J. Appl. Polym. Sci.* 28, 851.
- Hancock, T., 1857. *Personal Narrative of the Origin and Progress of the Caoutchouc or India-Rubber Manufacture in England*. Longman, Brown, Green, Longmans, and Roberts, London; reprinted (1920).
- Hands, D., 1980. *Rubber Chem. Technol.* 53, 80.
- Hansen, J.P., 1970. *Phys. Rev. A* 2, 221.

- Harwood, J.A.C., Payne, A.R., 1966a. *J. Appl. Polym. Sci.* 10, 315.
- Harwood, J.A.C., Payne, A.R., 1966b. *J. Appl. Polym. Sci.* 1203.
- Harwood, J.A.C., Schallamach, A., 1967. *J. Appl. Polym. Sci.* 11, 1835.
- Heinrich, G., Kluppel, M., Vilgis, T.A., 2002. *Curr. Opin. Sol. State Mater. Sci.* 6, 195.
- Hellwege, K.H., Knappe, W., Paul, F., Semjonow, V., 1967. *Rheol. Acta* 6, 165.
- Hess, W.M., 1991. *Rubber Chem. Technol.* 64, 386.
- Heymans, N., 2000. *Macromolecules* 33, 4226.
- Hiwatari, Y., Matsuda, H., Ogawa, T., Ogita, N., Ueda, A., 1974. *Prog. Theor. Phys.* 52, 1105.
- Hobbie, E.K., Fry, D.J., 2007. *J. Chem. Phys.* 126, 124907.
- Hoover, W.G., Ross, M., 1971. *Contemp. Phys.* 12, 339.
- Hosler, D., Burkett, S.L., Tarkanian, M.J., 1999. *Science* 284, 1988.
- Hsu, A.S., Leal, L.G., Non-Newt, J., 2009. *Fluid Mech.* 160, 176.
- Huppler, J.D., MacDonald, I.F., Ashare, E., Spriggs, T.W., Bird, R.B., Holmes, L.A., 1967. *J. Rheol.* 11, 181.
- Isono, Y., Obashi, N., Kase, T., 1995. *Macromolecules* 28, 5145.
- Isono, Y., Kamohara, T., Takano, A., Kase, T., 1997. *Rheol. Acta* 35, 245.
- Johnson, P.S., 2001. *Rubber Processing: An Introduction*. Hanser Publications.
- Kavassalis, T.A., Noolandi, J., 1989. *Macromolecules* 22, 2709.
- Kaye, A., 1962. Note to the College of Aeronautics. Cranfield, UK.
- Kennedy, A.J., 1953. *J. Mech. Phys. Solids* 1, 172.
- Knauss, W.G., Zhao, J., 2007. *Mech. Time-Depend. Mater.* 11, 199.
- Kohls, D.J., Beaucage, G., 2002. *Curr. Opin. Solid State Mater. Sci.* 6, 183.
- Kotliar, M., Kumar, R., Back, R.A., 1990. *J. Polym. Sci., Polym. Phys. Ed.* 28, 1033.
- Kramers, H.A., 1927. *Atti del Congresso Internazionale dei Fisici* 2, 545.
- Krause, S., Gormley, J.J., Roman, N., Shetter, J.A., Watanabe, W.H., 1965. *J. Polym. Sci. A* 3, 3573.
- Kremer, F., Schonhals, A. (Eds.), 2003. *Broadband Dielectric Spectroscopy*. Springer-Verlag, Berlin.
- Kronig, R. de L., 1926. *J. Opt. Soc. Am.* 12, 547.
- Laird, B.B., Haymet, A.D.J., 1992. *Mol. Phys.* 75, 71.
- Larson, R.G., 1985. *J. Rheol.* 29, 823.
- Larson, R.G., 1988. *Constitutive Equations for Polymer Melts and Solutions*. Butterworth, Boston.
- Larson, R.G., Valesano, V.A., 1986. *J. Rheol.* 30, 1093.
- Laun, H.M., 1986. *J. Rheol.* 30, 459.
- Leblans, P.J.R., Bastiaansen, C., 1989. *Macromolecules* 22, 3312.
- Lee, B.L., 1981. *Polym. Eng. Sci.* 21, 294.
- Le, H.H., Ilisch, S., Kasaliwal, G.R., Radosch, H.-J., 2008. *Rubber Chem. Technol.* 81, 767.
- Lin, Y.-H., 1987. *Macromolecules* 20, 3080.
- Lin, J.C., Hergenrother, W.L., Hilton, A.S., 2010. *J. Appl. Polym. Sci.* 115, 655.
- Lodge, T.P., 1999. *Phys. Rev. Lett.* 83, 3128.
- Lodge, A.S., Meissner, J., 1972. *Rheol. Acta* 11, 351.
- MacLean, D.L., 1973. *Trans. Soc. Rheol.* 17, 385.
- Macosko, C.W., 1994. *Rheology: Principles, Measurements, and Applications*. Wiley-VCH.
- Maiti, M., Bhattacharya, M., Bhowmick, A.K., 2008. *Rubber Chem. Technol.* 81, 384.
- March, N.H., Tosi, M.P., 2002. *Introduction to the Liquid State*. World Scientific, Singapore.
- Mark, J.E., 2006. *Accts. Chem. Res.* 39, 881.
- Marvin, R.S., 1953. In: Harrison, V.G.W. (Ed.), *Proc. 2nd Inter. Congress on Rheology*. Butterworths Sci. Pub., London.
- McCrum, N.G., Read, B.E., Williams, G., 1967. *Anelastic and Dielectric Effects in Polymer Solids*. Wiley, London.
- McKenna, G.B., Zapas, L.J., 1979. *J. Rheol.* 23, 151.
- McLean, D., 1966. *Rep. Prog. Phys.* 29, 1.
- Medalia, A.I., 1967. *J. Coll. Inter. Sci.* 24, 393.
- Medalia, A.I., 1972. *Rubber Chem. Technol.* 45, 1171.
- Medalia, A.I., 1986. *Rubber Chem. Technol.* 59, 432.
- Medalia, A.I., 1987. *Rubber Chem. Technol.* 60, 45.
- Menezes, E.V., Graessley, W.W., 1982. *J. Polym. Sci. Polym. Phys. Ed.* 20, 1817.
- Müllner, H.W., Ernst, G., Eberhardsteiner, J., 2008. *J. Appl. Polym. Sci.* 110, 76.

- Mihara, S., Datta, R.N., Noordermeer, J.W.M., 2009. *Rubber Chem. Technol.* 82, 524.
- Milner, S.T., 1996. *J. Rheol.* 40, 303.
- Moelwyn-Hughes, E.A., 1961. *Physical Chemistry*, second ed. Pergamon Press, NY.
- Monfort, J.P., Mann, G., Monge, P., 1984. *Macromolecules* 17, 1551.
- Montes, S., White, J.L., Nakajima, N., 1988. *J. Non-Newton. Fluid Mech.* 28, 183.
- Mooney, M., 1936. *Physics* 7, 413.
- Moore, J.D., Cui, S.T., Cochran, H.D., Cummings, P.T., 1999. *Phys. Rev. E* 60, 6956.
- Morton-Jones, D.H., 1989. *Polymer Processing*. Chapman & Hall.
- Mott, P.H., Roland, C.M., 1996. *Macromolecules* 29, 8492.
- Mott, P.H., Roland, C.M., 2009. *Phys. Rev. B* 80, 132104.
- Mullins, L., 1969. *Rubber Chem. Technol.* 42, 339.
- Nah, C., Lim, J.Y., Cho, B.H., Hong, C.K., Gent, A.N., 2010. *J. Appl. Polym. Sci.* 118, 1574.
- Nelson, C.J., Avgeropoulos, G.N., Weissert, F.C., Bohm, G.G.A., 1977. *Angew. Makro. Chem.* 60, 49.
- Nemoto, N., Moriwaki, M., Odani, H., Kurata, M., 1971. *Macromolecules* 4, 215.
- Nemoto, N., Odani, H., Kurata, M., 1972. *Macromolecules* 5, 531.
- Ngai, K.L., Schonhals, A., Schlosser, E., 1992. *Macromolecules* 25, 4915.
- Ngai, K.L., Plazek, D.J., Roland, C.M., 2008. *Macromolecules* 41, 3925.
- Ngai, K.L., Plazek, D.J., 1995. *Rubber Chem. Technol.* 68, 376.
- Nikiel, L., Wampler, W., Neilsen, J., Hershberger, N., 2009. *Rubber Plast. News*, p. 12.
- Oberhauser, J.P., Leal, L.G., Mead, D.W., 1998. *J. Polym. Sci. Polym. Phys. Ed.* 36, 265.
- Osswald, T.A., Gries, T., 2006. *Polymer Processing: Modeling and Simulation*. Hanser Gardner Publications.
- Palade, L.I., Verney, V., Attane, P., 1995. *Macromolecules* 28, 7051.
- Paluch, M., 2001. *J. Chem. Phys.* 115, 10029.
- Paluch, M., Roland, C.M., Best, A., 2002. *J. Chem. Phys.* 117, 1188.
- Paluch, M., Roland, C.M., Gapinski, J., Patkowski, A., 2003. *J. Chem. Phys.* 118, 3177.
- Pathak, J.A., Twigg, J.N., Nugent, K.E., Ho, D.L., Lin, E.K., Mott, P.H., Robertson, C.G., Vukmir, M.K., Epps, T.H., Roland, C.M., 2008. *Macromolecules* 41, 7543.
- Payne, A.R., 1962. *J. Appl. Polym. Sci.* 6, 57.
- Payne, A.R., 1963. *J. Appl. Polym. Sci.* 7, 873.
- Payne, A.R., 1964. *J. Appl. Polym. Sci.* 8, 2661.
- Peng, X., Huang, Y., Xia, T., Kong, M., Li, G., 2011. *Eur. Polym. J.* 47, 1956.
- Plazek, D.J., 1965. *J. Phys. Chem.* 6, 612.
- Plazek, D.J., 1980. *Polymer J.* 12, 43.
- Plazek, D.J., 1996. *J. Rheol.* 40, 987.
- Plazek, D.J., Ngai, K.L., 1991. *Macromolecules* 24, 1222.
- Plazek, D.J., O'Rourke, V.M., 1971. *J. Polym. Sci. B2* (9), 209.
- Plazek, D.J., Rosner, M.J., Plazek, D.L., 1988. *J. Polym. Sci. Polym. Phys.* 26, 473.
- Plazek, D.J., Seoul, C., Bero, C.A., Non-Cryst, J., 1991. *Solids* 131–133, 570.
- Plazek, D.J., Bero, C., Neumeister, S., Floudas, G., Fytas, G., Ngai, K.L., 1994. *Colloid. Polym. Sci.* 272, 1430.
- Plazek, D.J., Chay, I.-C., Ngai, K.L., Roland, C.M., 1995. *Macromolecules* 28, 6432.
- Pohl, H.A., Gogos, C.G., 1961. *J. Appl. Polym. Sci.* 5, 67.
- Rallison, J.M., 1984. *Ann. Rev. Fluid Mech.* 16, 45.
- Ram, A., Izrailov, L., 1986. *J. Appl. Polym. Sci.* 31, 85.
- Reader's Digest, 1958. *The Reader's Digest Assoc. Inc.*, Pleasantville, NY, January.
- Reiner, M., 1964. *Phys. Today* 17, 62.
- Richter, D., Farago, B., Butera, R., Fetters, L.J., Juang, J.S., Ewen, B., 1993. *Macromolecules* 26, 795.
- Robertson, C.G., Rademacher, C.M., 2004. *Macromolecules* 37, 10009.
- Robertson, C.G., Roland, C.M., 2008. *Rubber Chem. Technol.* 81, 506.
- Robertson, C.G., Wang, X., 2005. *Phys. Rev. Lett.* 95, 075703.
- Robertson, C.G., Roland, C.M., Puskas, J.E., 2002. *J. Rheol.* 46, 307.
- Robertson, C.G., Warren, S., Plazek, D.J., Roland, C.M., 2004. *Macromolecules* 37, 10018.
- Robertson, C.G., Bogoslovov, R., Roland, C.M., 2007. *Phys. Rev. E* 75, 051403.
- Robertson, C.G., Lin, C.J., Rackaitis, M., Roland, C.M., 2008. *Macromolecules* 41, 2727.
- Roland, C.M., 1989. *J. Rheol.* 33, 659.

- Roland, C.M., 1990. *J. Rheol.* 34, 25.
- Roland, C.M., 2010. *Macromolecules* 43, 7875.
- Roland, C.M., 2011. *Viscoelastic Behavior of Rubbery Materials*. Oxford University Press.
- Roland, C.M., Bohm, G.G.A., 1984. *J. Polym. Sci. Pt. B—Polym. Phys.* 22, 79.
- Roland, C.M., Bohm, G.G.A., 1985. *Macromolecules* 18, 1310.
- Roland, C.M., Nguyen, M., 1988. *J. Appl. Polym. Sci.* 35, 2141.
- Roland, C.M., Robertson, C.G., 2006. *Rubber Chem. Technol.* 79, 267.
- Roland, C.M., Ngai, K.L., Santangelo, P.G., Qiu, X.H., Ediger, M.D., Plazek, D.J., 2001. *Macromolecules* 34, 6159.
- Roland, C.M., Paluch, M., Casalini, R., 2004. *J. Polym. Sci. Polym. Phys. Ed.* 42, 4313.
- Roland, C.M., Robertson, C.G., Nikiel, L., Puskas, J.E., 2004. *Rubber Chem. Technol.* 77, 372.
- Roland, C.M., Ngai, K.L., Plazek, D.J., 2004. *Macromolecules* 37, 7051.
- Roland, C.M., Hensel-Bielowka, S., Paluch, M., Casalini, R., 2005. *Rep. Prog. Phys.* 68, 1405.
- Roland, C.M., Bair, S., Casalini, R., 2006. *J. Chem. Phys.* 125, 124508.
- Ronca, G., 1983. *J. Chem. Phys.* 79, 1031.
- Roovers, J., 1985. *Macromolecules* 8, 1359.
- Roovers, J., Toporowski, P.M., 1990. *Rubber Chem. Technol.* 63, 734.
- Rössler, E., 1990. *Phys. Rev. Lett.* 65, 1595.
- Rott, N., 1990. *Ann. Rev. Fluid Mech.* 22, 1.
- Royer, J.R., Gay, Y.J., Desimone, J.M., Khan, S.A., 2000. *J. Polym. Sci. Polym. Phys.* 38, 3168.
- Rudin, A., Schreiber, H.P., 1983. *Polym. Eng. Sci.* 23, 422.
- Sadhu, S., Bhowmick, A.K., 2003. *Rubber Chem. Technol.* 76, 860.
- Sampoli, M., Benassi, P., Eramo, R., Angelani, L., Ruocco, G., 2003. *J. Phys. Condens. Matter.* 15, S1227.
- Santangelo, P.G., Roland, C.M., 1998. *Macromolecules* 31, 3715.
- Santangelo, P.G., Roland, C.M., 2001. *J. Rheol.* 45, 583.
- Schach, R., Creton, C., 2008. *J. Rheol.* 52, 749.
- Schneider, U., Lunkenheimer, P., Brand, R., Loidl, A., 1999. *Phys. Rev. E* 59, 6924.
- Schug, K.U., King, H.E., Böhmer, R., 1998. *J. Chem. Phys.* 109, 1472.
- Schwartz, G.A., Cervený, S., Marzocca, A.J., Gerspacher, M., Nikiel, L., 2003. *Polymer* 44, 7229.
- Sengupta, R., Chakraborty, S., Bandyopadhyay, S., Dasgupta, S., Mukhopadhyay, R., Auddy, K., Deuri, A.S., 2007. *Polym. Eng. Sci.* 47, 1956.
- Shih, C.K., 1976. *Polym. Eng. Sci.* 16, 742.
- Sichel, E.K. (Ed.), 1982. *Carbon Black-Polymer Composites*. Marcell Dekker, New York.
- Simha, R., Boyer, R.F., 1962. *J. Chem. Phys.* 37, 1003.
- Simmons, J.M., 1968. *Rheol. Acta* 7, 184.
- Sirisinha, C., Saeoui, P., Guaysomboon, J., 2003. *J. Appl. Polym. Sci.* 90, 4038.
- Skewis, J.D., 1966. *Rubber Chem. Technol.* 39, 217.
- Skorodumov, V.F., Godovskii, Y.K., 1993. *Polym. Sci.* 35, 562.
- Stankovich, S., Dikin, D.A., Dommett, G.H.B., Kohlhaas, K.M., Zimney, E.J., Stach, E.A., Piner, R.D., Nguyen, S.T., Ruoff, R.S., 2006. *Nature* 442, 282.
- Stillinger, F.H., Weber, T.A., 1984. *Science* 225, 983.
- Stillinger, H., Debenedetti, P.G., Truskett, T.M., 2001. *J. Phys. Chem. B* 105, 11809.
- Stratton, R.A., Butcher, A.F., 1973. *J. Polym. Sci. Polym. Phys. Ed.* 11, 1747.
- Tadmor, Z., Gogos, C.G., 2006. *Principles of Polymer Processing*, second ed. Wiley-Interscience.
- Tanner, R.I., 1970. *J. Polym. Sci. Polym. Phys. Ed.* 8, 2067.
- Tanner, R.I., 1988. *J. Rheol.* 32, 673.
- Tanner, R.I., Williams, G., 1971. *Rheol. Acta* 10, 528.
- Tschoegl, N.W., 1989. *The Phenomenological Theory of Linear Viscoelastic Behavior*. Springer-Verlag, Berlin.
- Turner, D.T., 1978. *Polymer* 19, 789.
- Ueberreiter, K., Kanig, G., 1952. *J. Colloid Sci.* 7, 569.
- Valadares, L.F., Leite, C.A.P., Galembeck, F., 2006. *Polymer* 47, 672.
- Van Krevelen, D.W., 1990. *Properties of Polymers*. Elsevier, Amsterdam.
- Venerus, D.C., Schieber, J.D., Iddir, H., Guzman, J.D., Broerman, A.W., 1999. *Phys. Rev. Lett.* 82, 366.
- Vinogradov, G.V., Belkin, I.M., 1965. *J. Polym. Sci.* A3, 917.
- Vrentas, J.S., Venerus, D.C., Vrentas, C.M., 1991. *J. Polym. Sci. Polym. Phys. Ed.* 29, 537.

- Vu, Y.T., Mark, J.E., Pham, L.H., Engelhardt, M., 2001. *J. Appl. Polym. Sci.* 82, 1391.
- Waddell, W.H., Evans, L.R., 1996. *Rubber Chem. Technol.* 69, 377.
- Wakabayashi, K., Pierre, C., Dikin, D.A., Ruoff, R.S., Ramanathan, T., Brinson, L.C., Torkelson, J.M., 2008. *Macromolecules* 41, 1905.
- Wang, S.Q., Poly, J., 2003. *Sci. Poly. Phys. Ed.* 41, 1589.
- Wang, X., Robertson, C.G., 2005. *Phys. Rev. E* 72, 031406.
- Watanabe, H., 1999. *Prog. Polym. Sci.* 24, 1253.
- Watanabe, H., Sakamoto, T., Kotaka, T., 1995. *Macromolecules* 18, 1008.
- Weber, W., 1835. *Ann. Phys. Chem.* 34, 247; 54, 1 (1841).
- Wendt, C.J., Cyphers, A., 2008. *J. Anthropol. Archaeol.* 27, 175.
- White, J.L., 1995. *Rubber Processing: Technology, Materials, and Principles*. Epic Press, Hanser Publications.
- Whittle, M., Dickinson, E., 1997. *Mol. Phys.* 90, 739.
- Widen, B., 1967. *Science* 157, 375.
- Widom, B., 1999. *Physica A* 263, 500.
- Williams, E., Angell, C.A., 1977. *J. Phys. Chem.* 81, 2323.
- Williams, M.L., Landel, R.F., Ferry, J.D., 1955. *Am. J. Chem. Soc.* 77, 3701.
- Wubbenhorst, M., Van Turnhout, J., *J. Non-Cryst. Solids* 305, 40.
- Xu, Y.Z., Dekee, D., Fong, C.F.C.M., 1995. *J. Appl. Polym. Sci.* 55, 779.
- Xu, X., Tao, X., Gao, C., Zheng, Q., 2008. *J. Appl. Polym. Sci.* 107, 1590.
- Yamaguchi, M., Gogos, C.G., 2001. *Adv. Polym. Test.* 20, 261.
- Yamane, M., Hirose, Y., Adachi, K., 2005. *Macromolecules* 38, 10686.
- Yannas, I.V., *J. Polymer Sci.* 1974. *Macro. Rev.* 9, 163.
- Ye, X., Tain, M., Xin, Y., Zhang, L.-Q., 2012. *J. Appl. Polym. Sci.* 124, 927.
- Zallen, R., 1981. *The Physics of Amorphous Solids*. Wiley, New York.